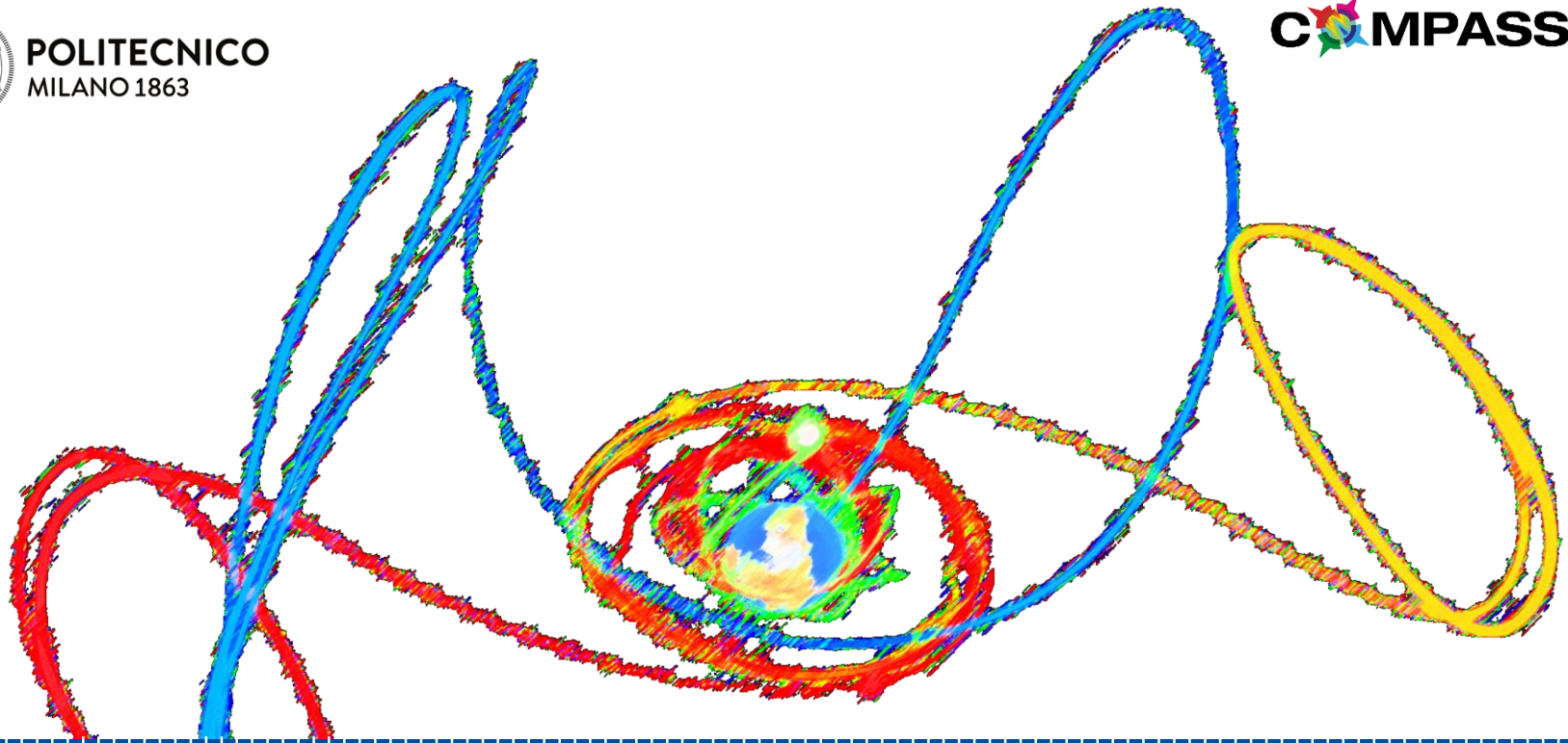




POLITECNICO
MILANO 1863



Luni-solar perturbations for missions design in highly elliptical orbits

Camilla Colombo

CNES HEO workshop 31 March 2017



INTRODUCTION

Highly Elliptical Orbits

Why highly elliptical Orbits

- Astrophysics and astronomy missions (e.g., INTEGRAL and XMM-Newton)
- Earth missions (e.g., Molniya or Tundra orbits, Drim constellation, magnetotail mission)
- Geostationary transfer orbits

Selection criteria

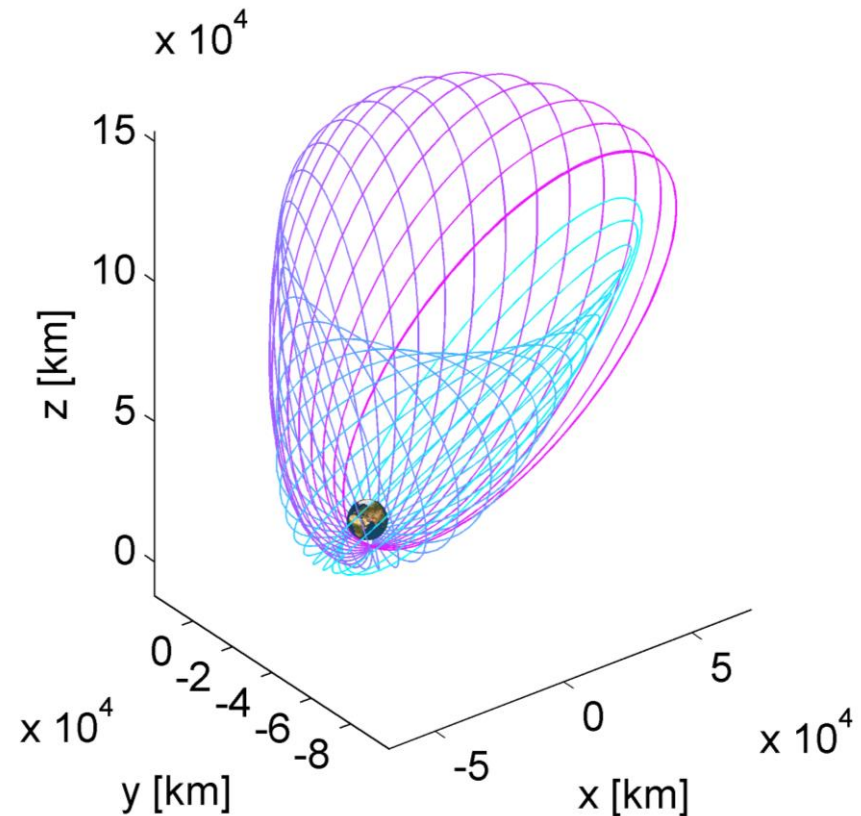
- Vantage points for the observation of the Earth and the Universe
- Avoid noise from radiation effects
- Geo-synchronicity to meet coverage requirements
- Inclination to minimise eclipse period

Highly Elliptical Orbits

...Fascinating interaction between third body luni-solar perturbation and Earth's oblateness

...Perfect example on how we can leverage the natural dynamical effect through manoeuvres to obtain free long-term effect on the orbit:

- Frozen orbits
- End-of-life Earth re-entry
- End-of-life graveyard orbit injection



Outline

- Dynamical model
- Analytical interpretation
- Dynamical maps
- Engineering Perturbation effects
- Applications



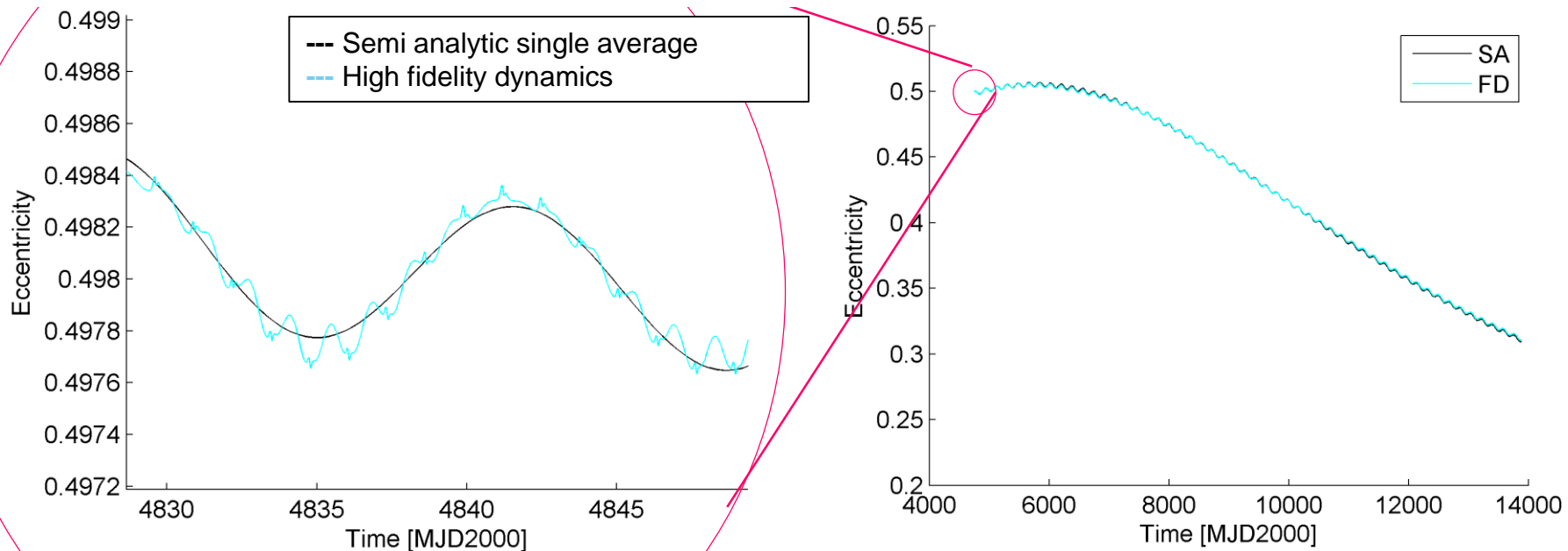
DYNAMICAL MODEL

Dynamical model

Orbit propagation based on averaged dynamics

Average variation of orbital elements over one orbit revolution

- Filter high frequency oscillations
- Reduce stiffness of the problem
- Decrease computational time for long term integration



Dynamical model

PlanODyn suite



Space Debris Evolution, Collision risk, and Mitigation
FP7/EU Marie Curie grant 302270



End-Of-Life Disposal Concepts for Lagrange-Point, Highly Elliptical Orbit missions, **ESA GSP**

End-Of-Life Disposal Concepts Medium Earth Orbit missions, **ESA GSP**



GEO disposal in “Revolutionary Design of Spacecraft through Holistic Integration of Future Technologies”
ReDSHIFT, H2020



COMPASS, ERC “Control for orbit manoeuvring through perturbations for supplication to space systems”

Dynamical model

Orbit propagation based on averaged dynamics

For conservative orbit perturbation effects

Disturbing potential function

$$R = R_{\text{SRP}} + R_{\text{zonal}} + R_{3\text{-Sun}} + R_{3\text{-Moon}}$$

Planetary equations in Lagrange form

$$\frac{d\mathbf{a}}{dt} = f\left(\mathbf{a}, \frac{\partial R}{\partial \mathbf{a}}\right) \quad \mathbf{a} = [a \quad e \quad i \quad \Omega \quad \omega \quad M]^T$$



Average over one orbit revolution of the spacecraft around the primary planet

$$\bar{R} = \bar{R}_{\text{SRP}} + \bar{R}_{\text{zonal}} + \bar{R}_{3\text{-Sun}} + \bar{R}_{3\text{-Moon}}$$

$$\frac{d\bar{\mathbf{a}}}{dt} = f\left(\bar{\mathbf{a}}, \frac{\partial \bar{R}}{\partial \bar{\mathbf{a}}}\right)$$

Single average



Average over the revolution of the perturbing body around the primary planet

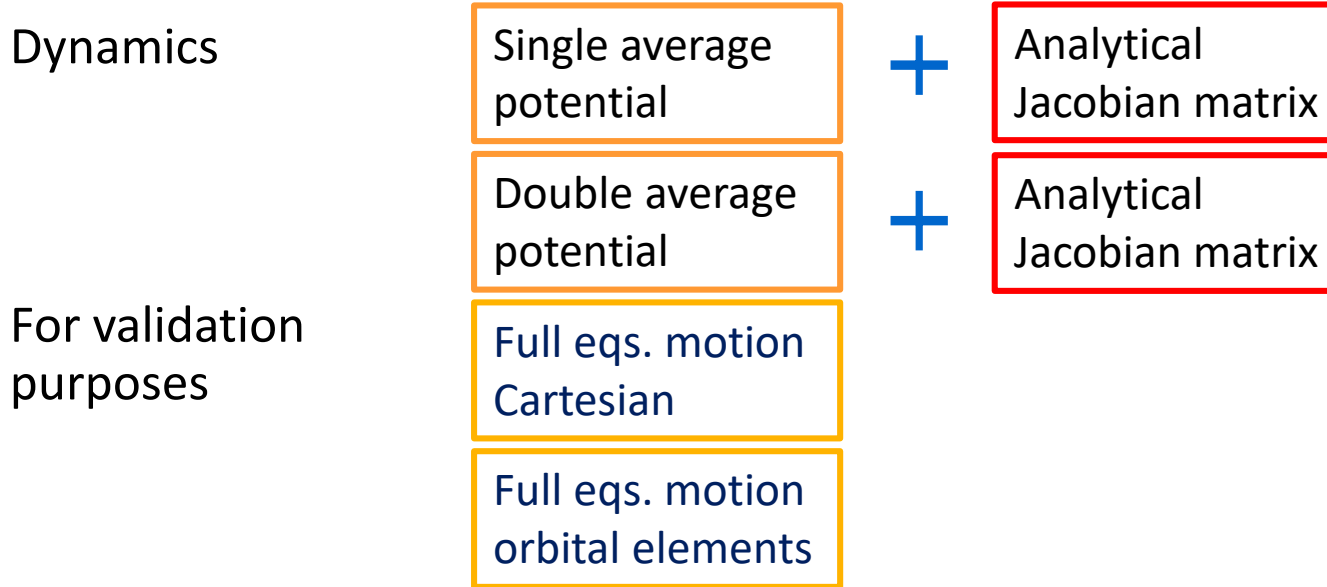
$$\bar{\bar{R}} = \bar{\bar{R}}_{\text{SRP}} + \bar{\bar{R}}_{\text{zonal}} + \bar{\bar{R}}_{3\text{-Sun}} + \bar{\bar{R}}_{3\text{-Moon}}$$

$$\frac{d\bar{\bar{\mathbf{a}}}}{dt} = f\left(\bar{\bar{\mathbf{a}}}, \frac{\partial \bar{\bar{R}}}{\partial \bar{\bar{\mathbf{a}}}}\right)$$

Double average

Dynamical model

PlanODyn: Planetary Orbital Dynamics



Integration method: explicit Runge-Kutta (4,5) method, Dormand-Prince pair

Implemented in Matlab

► Colombo C. "Planetary Orbital Dynamics Suite for Long Term Propagation in Perturbed Environment," ICATT, ESA/ESOC, 2016.

Dynamical model

Perturbation model

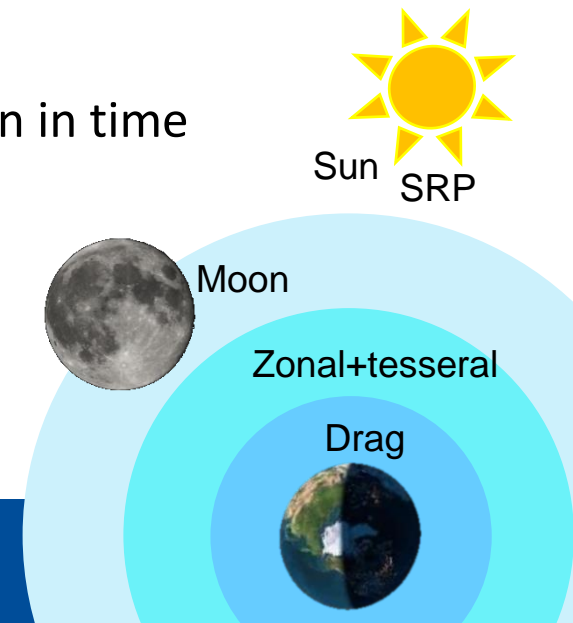
Perturbations in planet centred dynamics

- Atmospheric drag (piece-wise exponential model)
- Zonal harmonics of the Earth's gravity potential, J_2^2
- Solar radiation pressure (with eclipses)
- Third body perturbation of the Sun
- Third body perturbation of the Moon

Ephemerides options

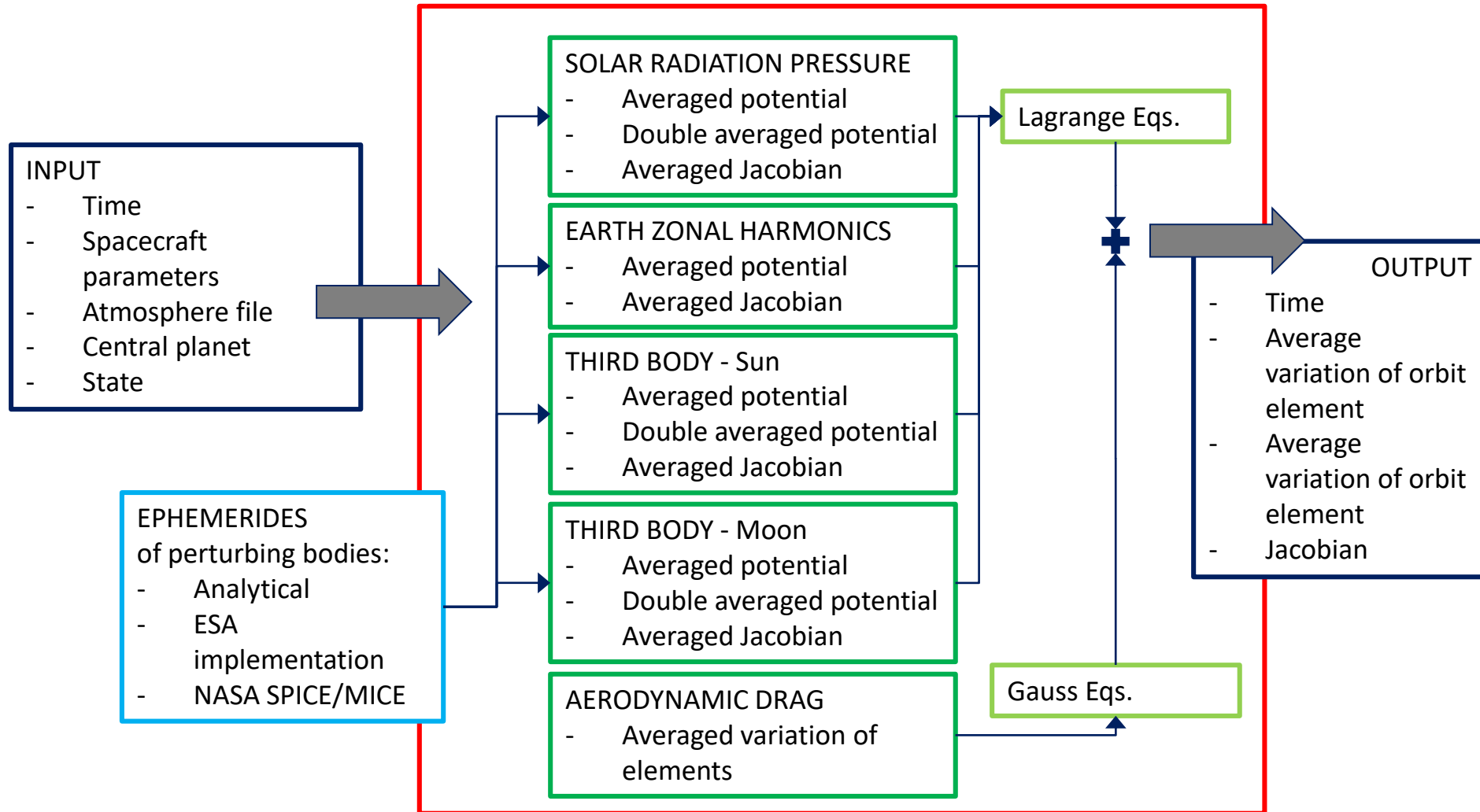
- Analytical approximation based on polynomial expansion in time
- Numerical ephemerides through the NASA SPICE toolkit
- Numerical ephemerides from an ESA implementation

Orbital elements in Earth centred equatorial J2000 frame



Dynamical model

PlanODyn: Planetary Orbital Dynamics



Third body potential

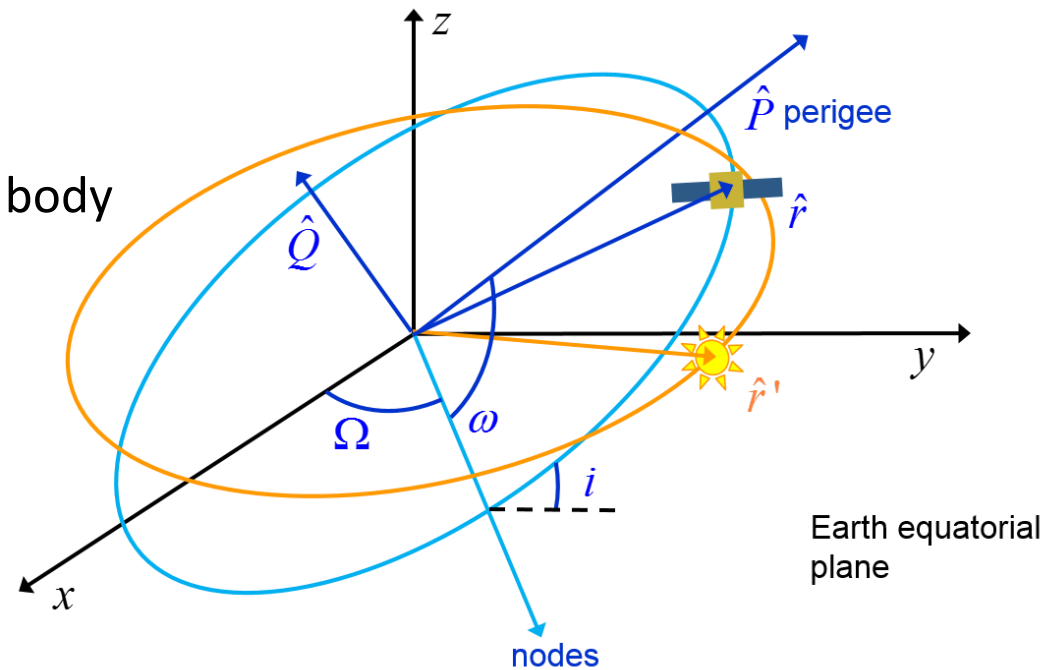
$$R_{3B}(r, r') = \frac{\mu'}{r'} \left(\left(1 - 2 \frac{r}{r'} \cos \psi + \left(\frac{r}{r'} \right)^2 \right)^{-1/2} - \frac{r}{r'} \cos \psi \right)$$

μ' gravitational coefficient of the third body

r' position vector of third body

r position vector of satellite

ψ angle between satellite and third body



Third body potential

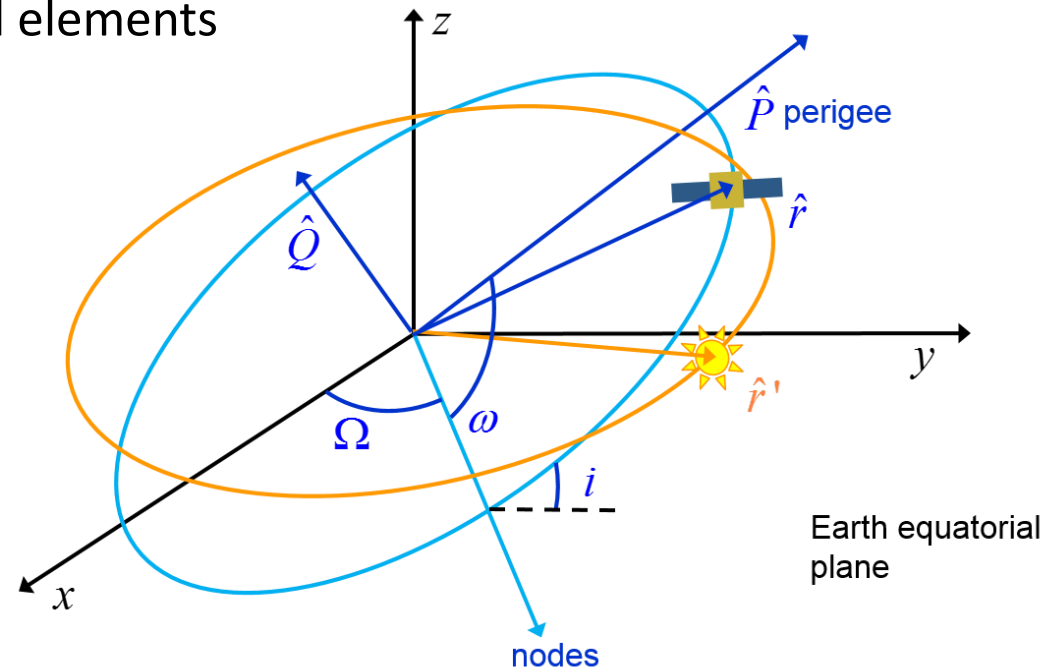
Third body potential in terms of:

- Ratio between orbit semi-major axis and distance of the third body $\delta = \frac{a}{r'}$
- Orientation of orbit eccentricity vector with respect to third body $A = \hat{P} \cdot \hat{r}'$
- Orientation of semi-latus rectum vector with respect to third body $B = \hat{Q} \cdot \hat{r}'$
- Composition of rotation in orbital elements

$$\hat{P} = R_3(\Omega)R_1(i)R_3(\omega) \cdot [1 \ 0 \ 0]^T$$

$$\hat{Q} = R_3(\Omega)R_1(i)R_3(\omega + \pi/2) \cdot [1 \ 0 \ 0]^T$$

$$\hat{r}' = R_3(\Omega')R_1(i')R_3(\omega' + f') \cdot [1 \ 0 \ 0]^T$$



Third body potential

Series expansion around $\delta = 0$

$$R_{3B}(r, r') = \frac{\mu'}{r'} \sum_{k=2}^{\infty} \delta^k F_k(A, B, e, E)$$

μ' gravitational coefficient of the third body

r' position vector of third body

E eccentric anomaly

Average over one orbit revolution

$$\bar{R}_{3B}(r, r') = \frac{\mu'}{r'} \sum_{k=2}^{\infty} \delta^k \bar{F}_k(A, B, e)$$

$$\bar{F}_k(A, B, e) = \frac{1}{2\pi} \int_{-\pi}^{\pi} F_k(A, B, e, E) \overbrace{(1 - e \cos E)}^{dM} dE$$

Partial derivatives for Lagrange equations

$$A(\Omega, i, \omega, \Omega', i', u')$$

$$B(\Omega, i, \omega, \Omega', i', u')$$

$$\bar{F}_k(A, B, e)$$



$$\frac{\partial \bar{F}_k}{\partial \Omega} = \frac{\partial \bar{F}_k}{\partial A} \frac{\partial A}{\partial \Omega} + \frac{\partial \bar{F}_k}{\partial B} \frac{\partial B}{\partial \Omega}$$

$$\frac{\partial \bar{F}_k}{\partial i} = \frac{\partial \bar{F}_k}{\partial A} \frac{\partial A}{\partial i} + \frac{\partial \bar{F}_k}{\partial B} \frac{\partial B}{\partial i}$$

$$\frac{\partial \bar{F}_k}{\partial \omega} = \frac{\partial \bar{F}_k}{\partial A} \frac{\partial A}{\partial \omega} + \frac{\partial \bar{F}_k}{\partial B} \frac{\partial B}{\partial \omega}$$

$$\frac{\partial \bar{F}_k}{\partial a} = \frac{k}{a} F_k$$

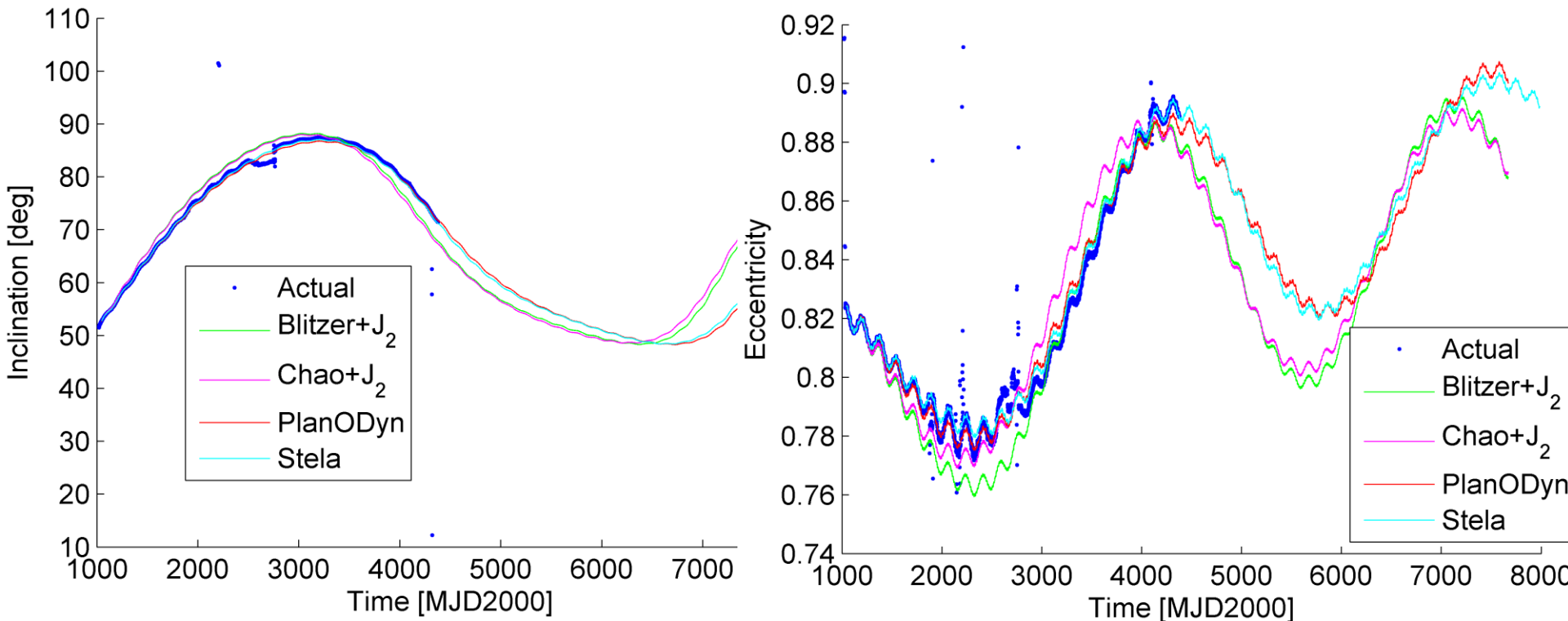
$$\frac{\partial \bar{F}_k}{\partial e}$$

► Kaufman and Dasenbrock, NASA report, 1979

Dynamical model

Order of the luni-solar potential expansion

Third-body perturbing potential of the Moon at least up to the fourth order of the power expansion



- ▶ *Blitzer L., Handbook of Orbital Perturbations, Astronautics, 1970*
- ▶ *Chao-Chun G. C., Applied Orbit Perturbation and Maintenance, 2005*

Dynamical model

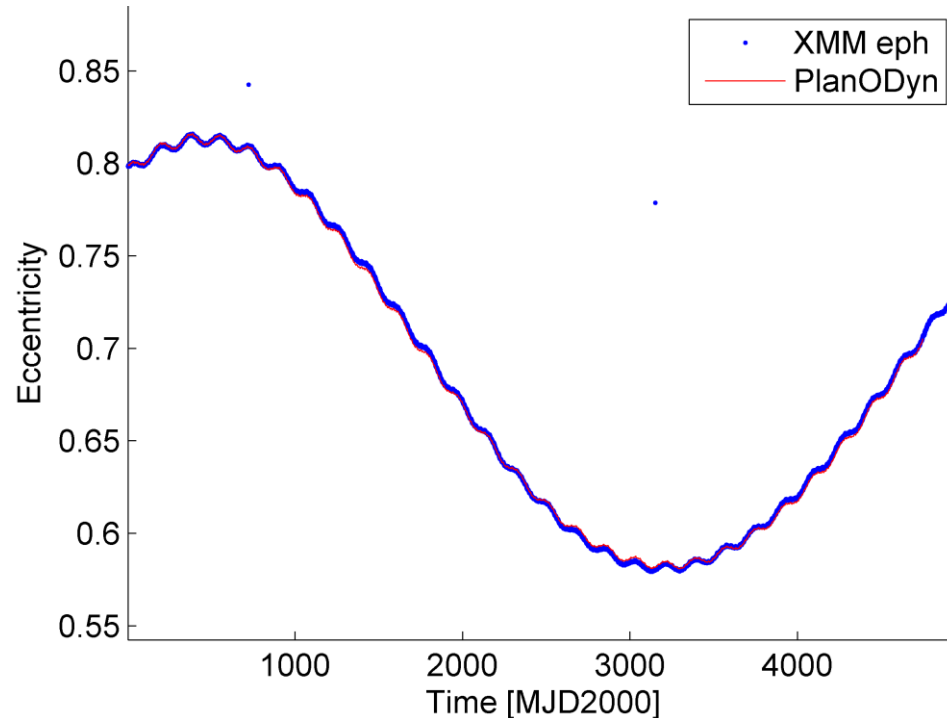
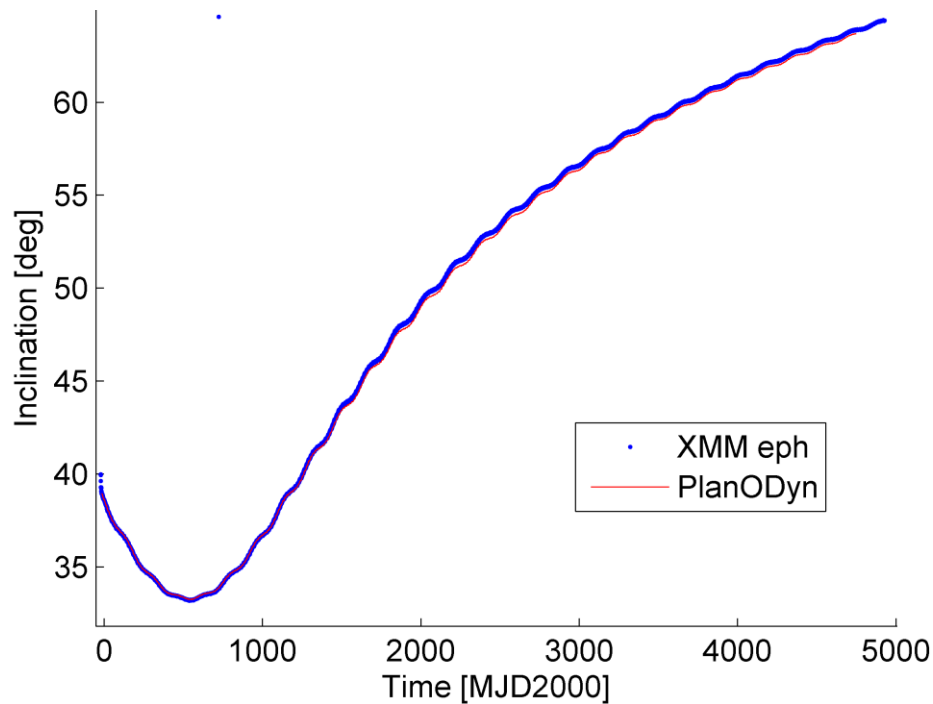
Validation: XMM Newton trajectory

Propagation time: 1999/12/15 to 2013/01/01

Initial Keplerian elements from ESA on 1999/12/15 at 15:00:

$a = 67045$ km, $e = 0.7951$, $i = 0.67988$ rad, $\Omega = 4.1192$ rad, $\omega = 0.99259$ rad

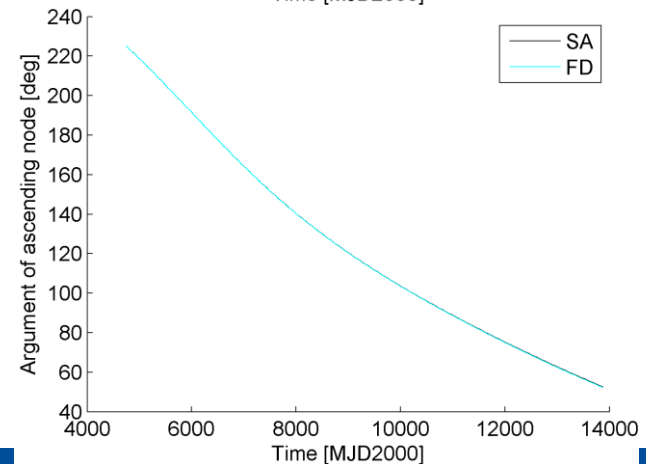
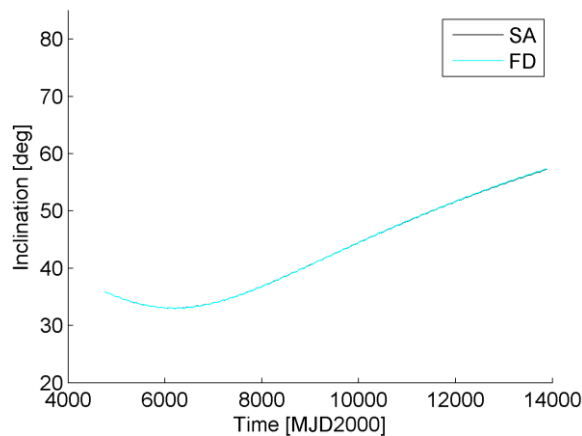
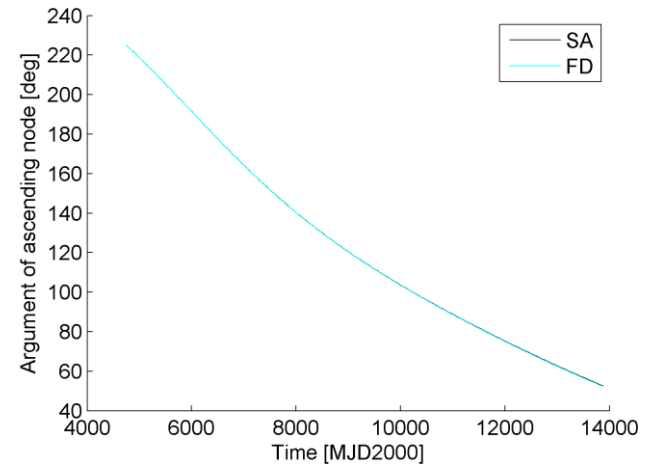
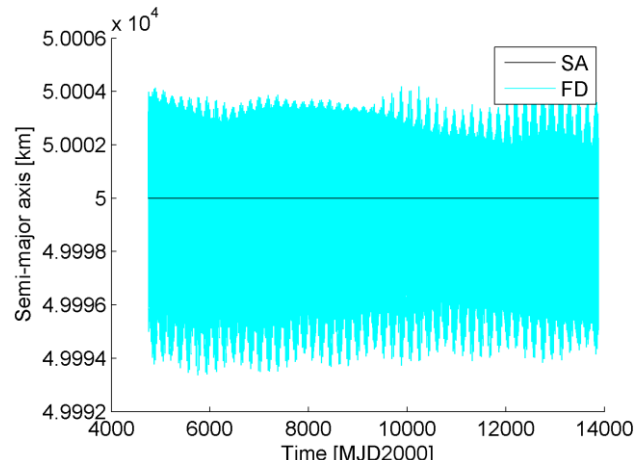
System: Earth centred, equatorial J2000



Dynamical model

Mean vs high fidelity dynamics

Initial Keplerian elements: $a = 50000$ km, $e = 0.5$, $i = 35.88$ deg, $\Omega = 225$ deg, $\omega = 63.9$ deg





ANALYTICAL INTERPRETATION

Third-body double averaged potential

Double averaging over one orbit revolution of the s/c and one orbit evolution of the perturbing body (either Sun or Moon) around the Earth

$$\bar{\bar{R}}_{3B}(r, r') = \frac{\mu'}{r'} \sum_{k=2}^{\infty} \delta^k \bar{\bar{F}}_k(e, i, \Omega, \omega, i')$$

Earth's centred equatorial reference system.

Same approach as El'yasberg (and Kozai) with some improvements:

- Avoid simplification that Moon and Sun orbit on the same plane (very important for precise orbit evolution)
- Facilitate the introduction of the effect of the zonal harmonics

$$\bar{\bar{F}}_k(e, i, \Delta\Omega, \omega, i') = \frac{1}{2\pi} \int_0^{2\pi} \bar{F}_k(A(\Omega, i, \omega, \Omega', i', \omega' + f'), B(\Omega, i, \omega, \Omega', i', \omega' + f'), e) df'$$

► *Kozai, Secular Perturbations of Asteroids with High Inclination and Eccentricity, 1962*

► *El'yasberg, Introduction to the theory of flight of artificial Earth satellites - translated, 1967*

Third body Kozai theory

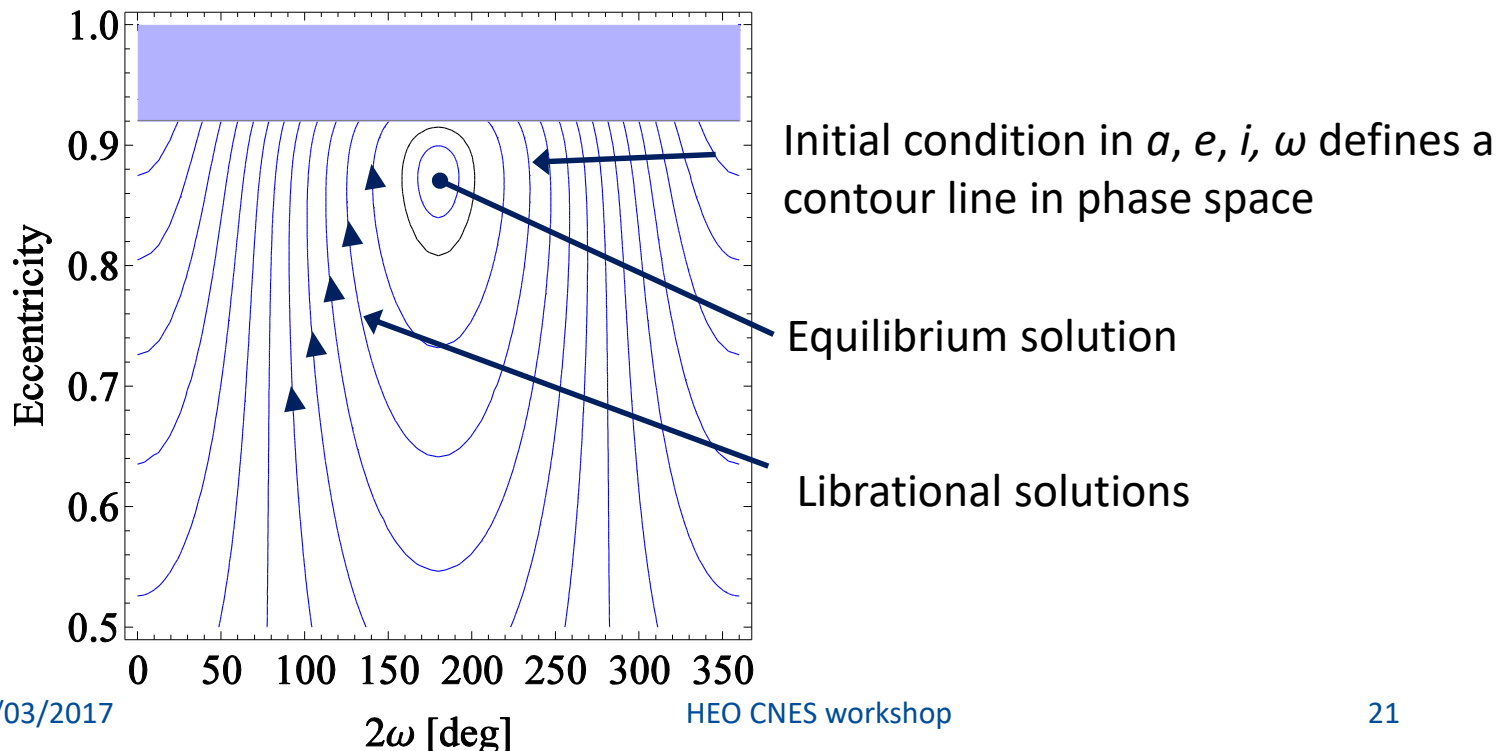
- Delaunay's transformation
- Time-independent Hamiltonian
- Double averaged potential
- Rotating reference system

$$W\left(\frac{a}{a'}, \Theta, e, 2\omega\right) = \text{const} \quad \Theta = (1 - e^2) \cos i^2$$

$$\bar{F}_{3\text{Bsys},2}(e, \omega, i) = \frac{1}{32} \left((2 + 3e^2)(1 + 3\cos(2i)) + 30e^2 \cos(2\omega) \sin^2 i \right)$$

► *Kozai, Secular Perturbations of Asteroids with High Inclination and Eccentricity, 1962*

► *El'yasberg, Introduction to the theory of flight of artificial Earth satellites - translated, 1967*



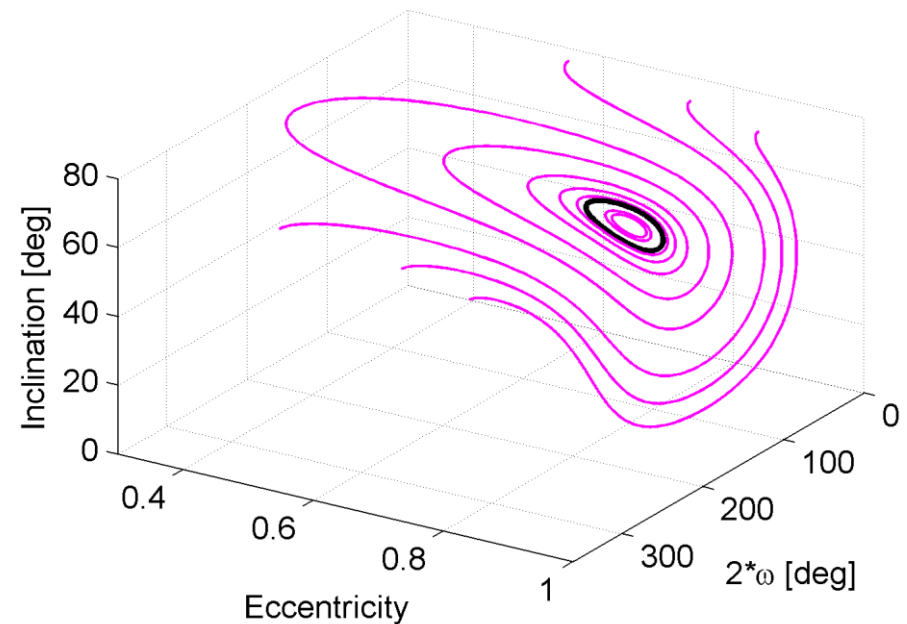
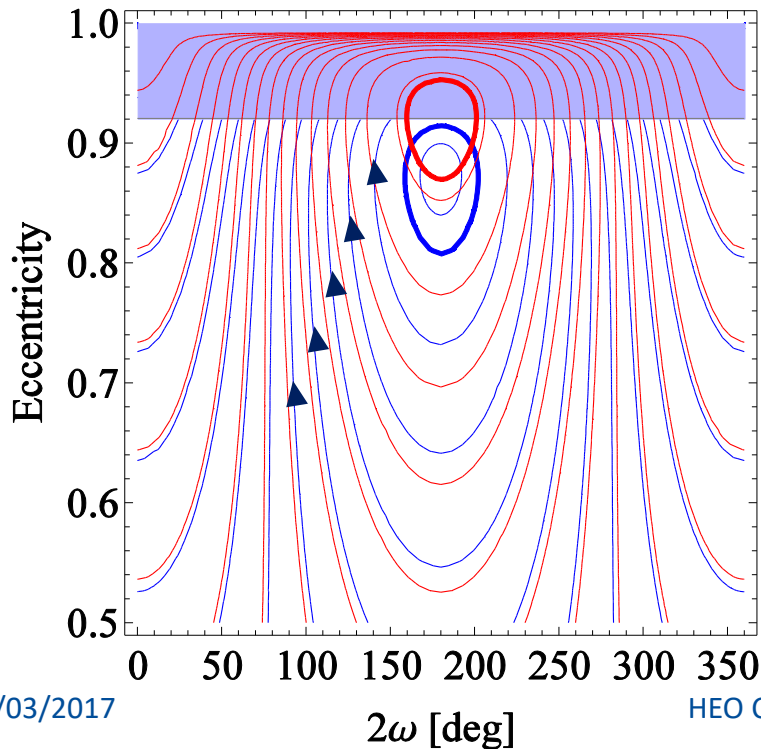
Analytical interpretation

Third body Kozai theory

$$W\left(\frac{a}{a'}, \Theta, e, 2\omega\right) = \text{const} \quad \Theta = (1 - e^2) \cos i^2$$

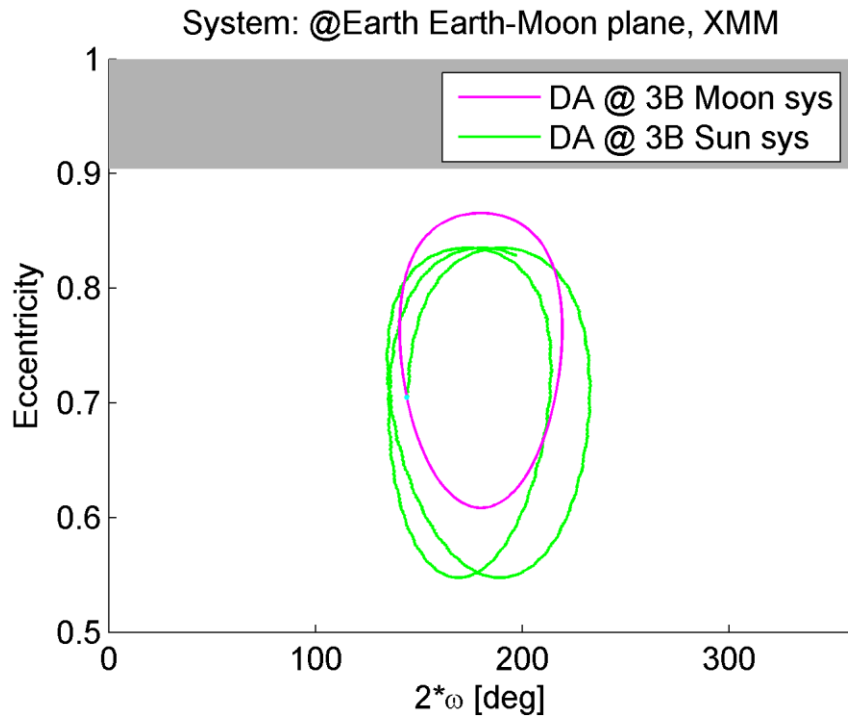
a/a' increases

\ominus decreases



Analytical interpretation

Third-body double averaged potential



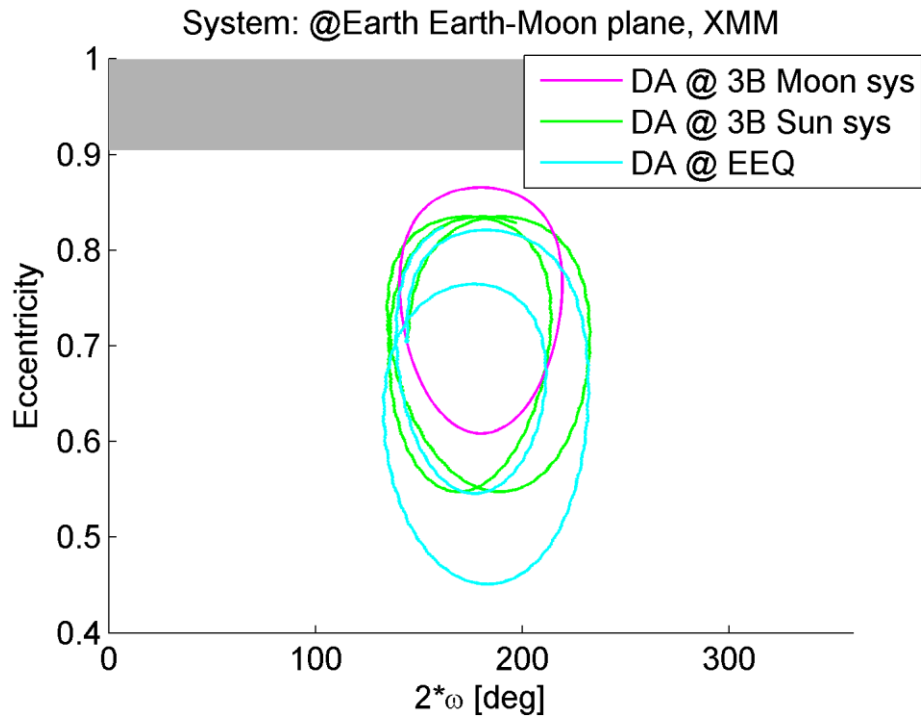
Reference system for figure:

- x-y plane lays on the Moon orbital plane
- z-axis in the direction of the Moon angular momentum

Kozai, El'yasberg: $\bar{\bar{F}}_{3\text{Bsys},2}(e, \omega, i)$

Analytical interpretation

Third-body double averaged potential



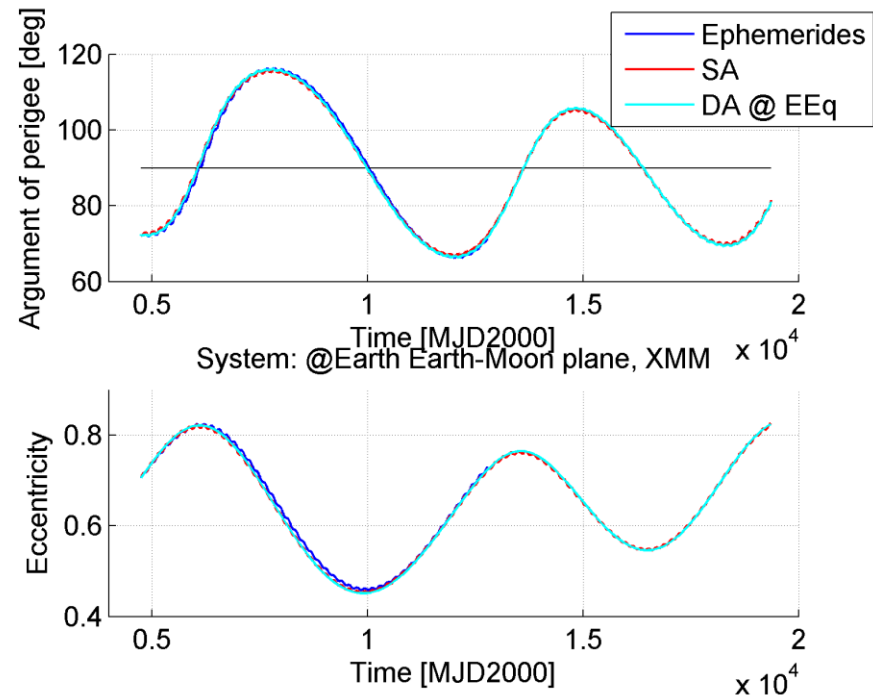
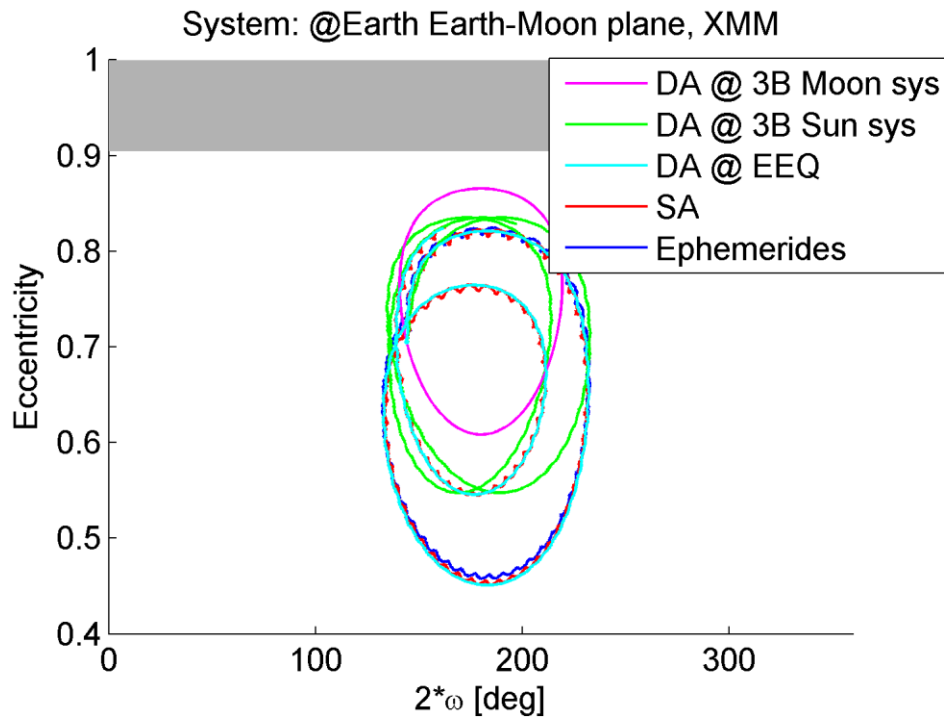
Kozai, El'yasberg: $\bar{\bar{F}}_{3\text{Bsys},2}(e, \omega, i)$



$\bar{\bar{F}}_k(e, i, \Delta\Omega, \omega, i')$

Analytical interpretation

Third-body double averaged potential



Kozai, El'yasberg: $\bar{\bar{F}}_{3\text{Bsys},2}(e, \omega, i)$



$\bar{\bar{F}}_k(e, i, \Delta\Omega, \omega, i')$

Non autonomous loops in the e - ω phase space!



DYNAMICAL MAPS

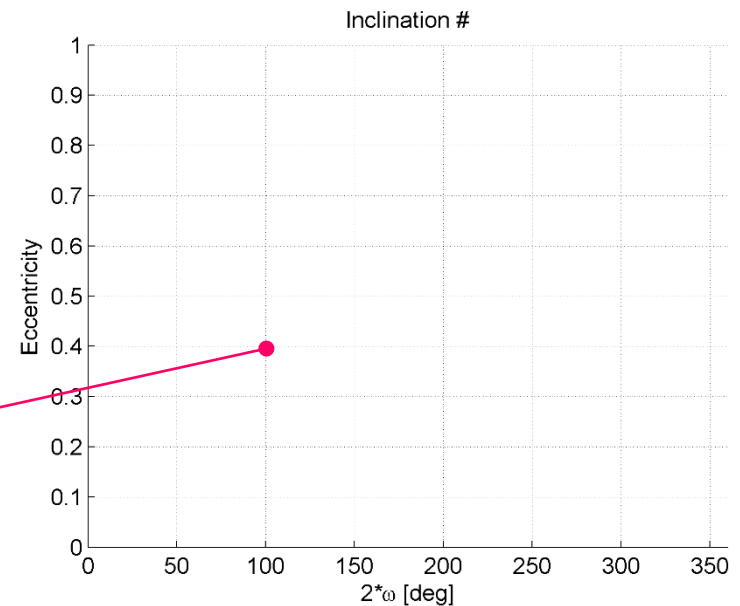
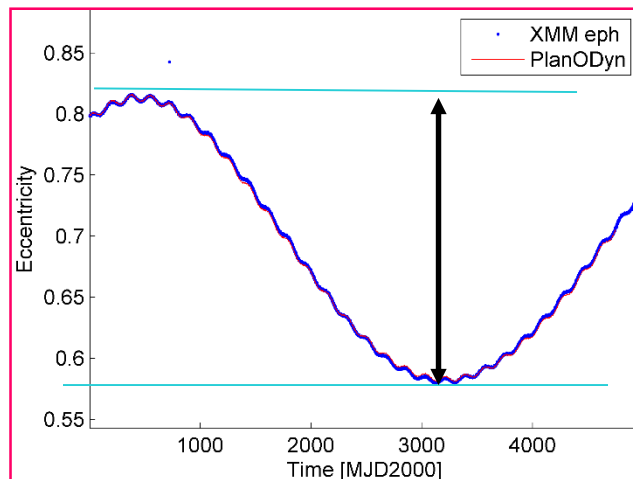
Long-term orbit evolution

1. Grid in inclination, eccentricity and ω (Moon plane reference system)
2. Propagation over ± 30 years with PlanODyn
3. Evaluate

$$\Delta e = e_{\max} - e_{\min}$$

$$e_{\max} = \max_t e(t) \quad t \in \left[-\Delta t_{\text{graveyard}} \quad +\Delta t_{\text{graveyard}} \right]$$

$$e_{\min} = \min_t e(t) \quad t \in \left[-\Delta t_{\text{graveyard}} \quad +\Delta t_{\text{graveyard}} \right]$$



Long-term orbit evolution

Luni-solar + zonal Δe maps

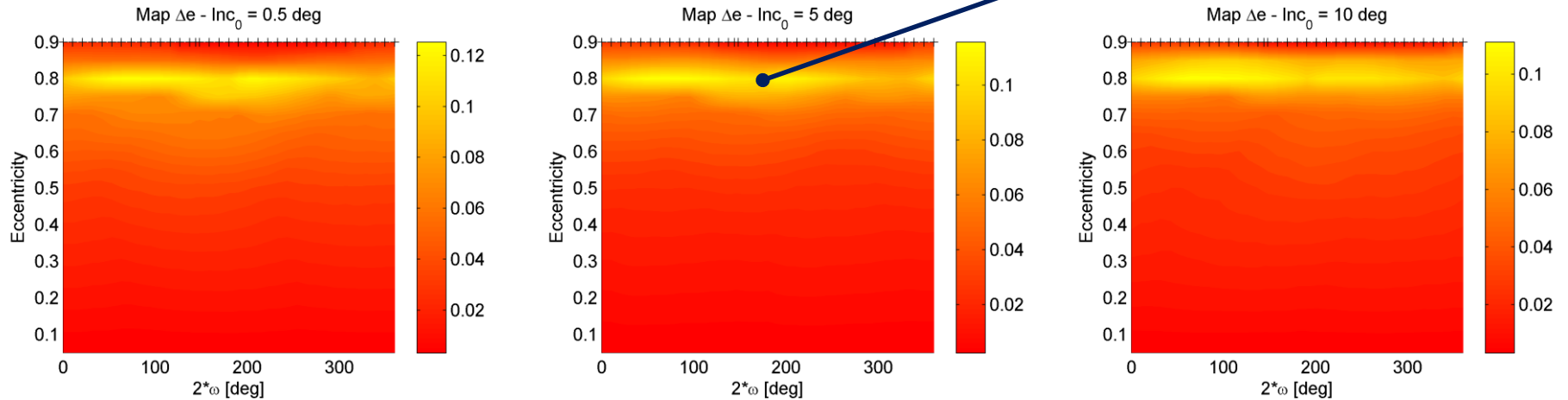
- Semi-major axis equal to 67045.39 km (XMM Newton's orbit)
- Different values of initial inclination with respect to the orbiting plane of the Moon
- Here: fixed t_0 and fixed Ω_0 to analyse one loop in the phase space but different Ω_0 can be taken into account with $2\omega + \Omega_0$

► Colombo C. "Long-Term Evolution of Highly-Elliptical Orbits: Luni-Solar Perturbation Effects for Stability and Re-Entry,"
25th AAS/AIAA Space Flight Mechanics Meeting, 2015

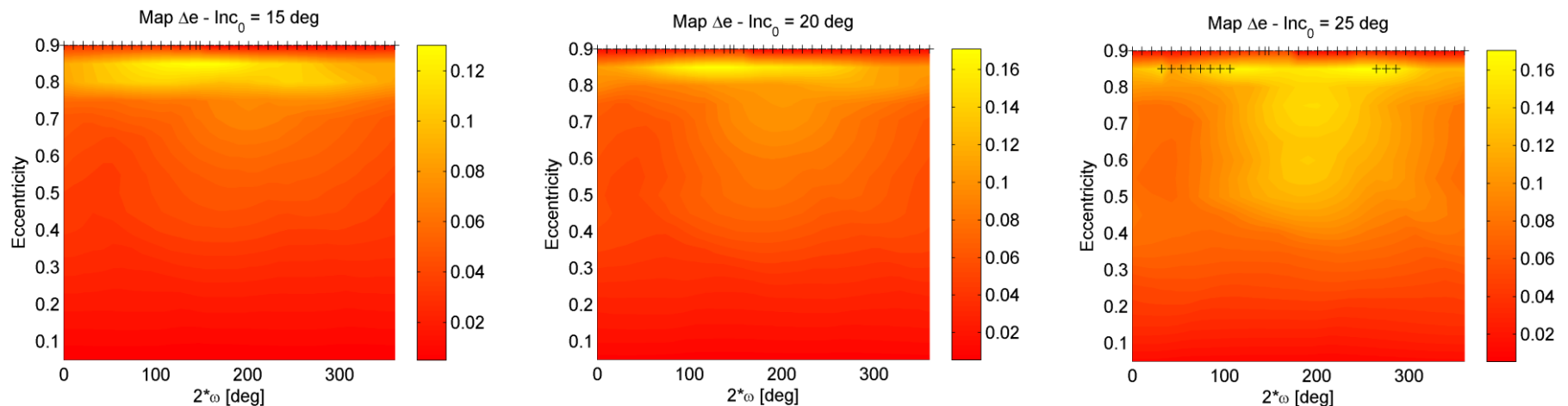
Dynamical maps

Long-term orbit evolution

Higher Δe variation for high initial e



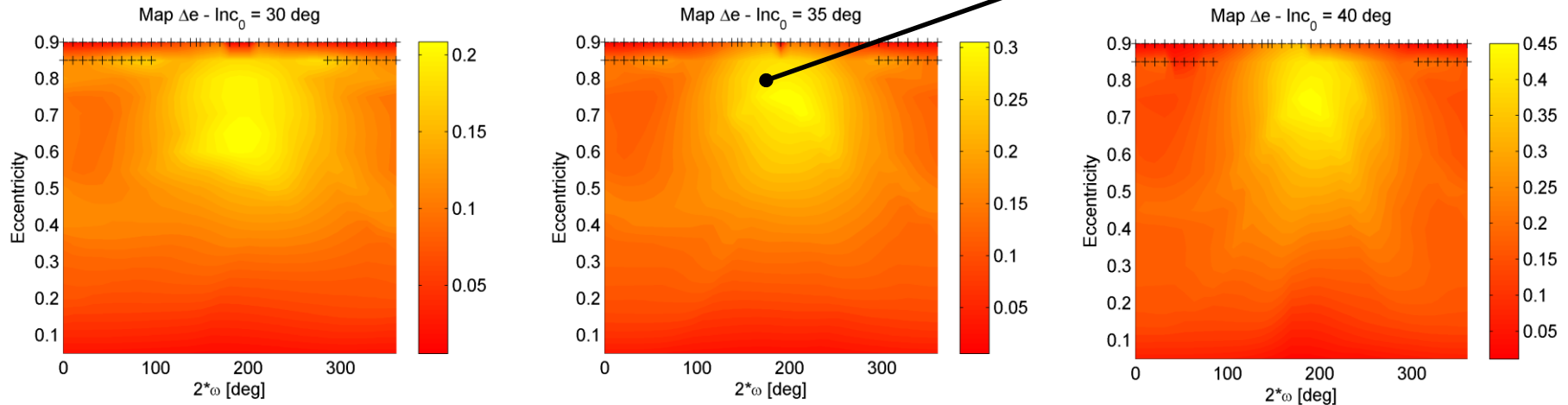
Rotational solutions in ω



Dynamical maps

Long-term orbit evolution

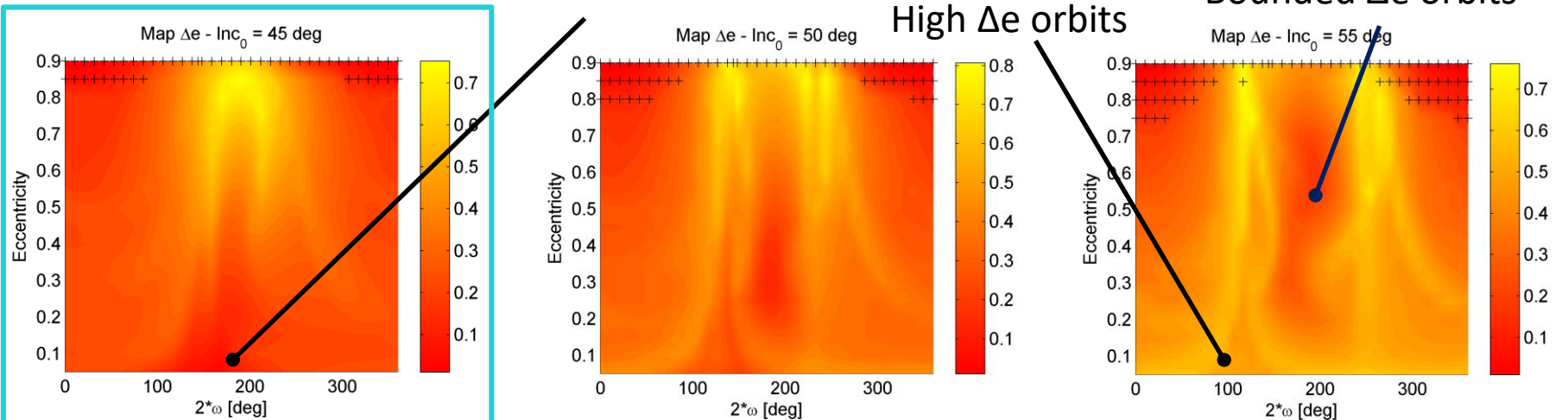
Higher Δe variation for high initial e



Low Δe orbits

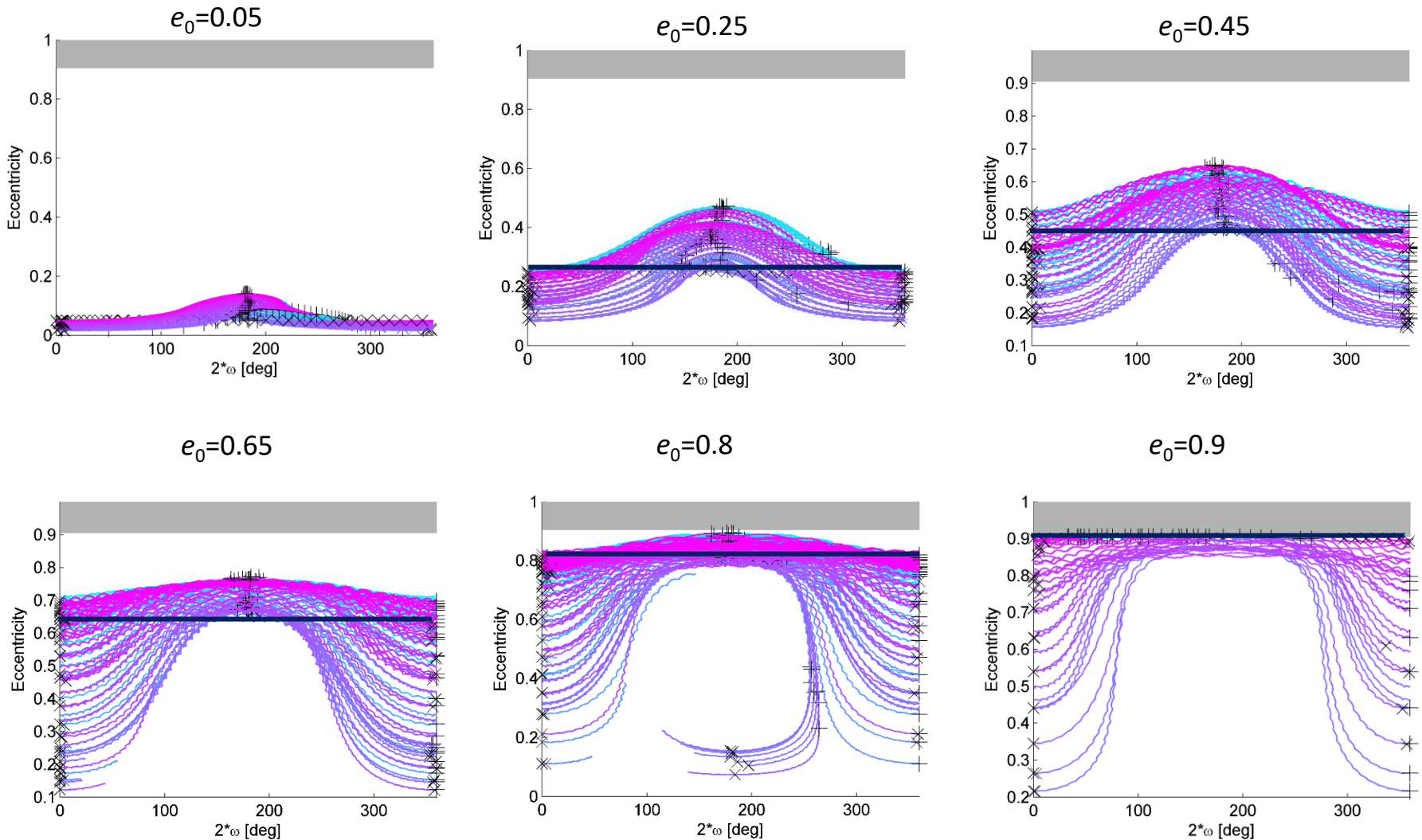
High Δe orbits

Bounded Δe orbits



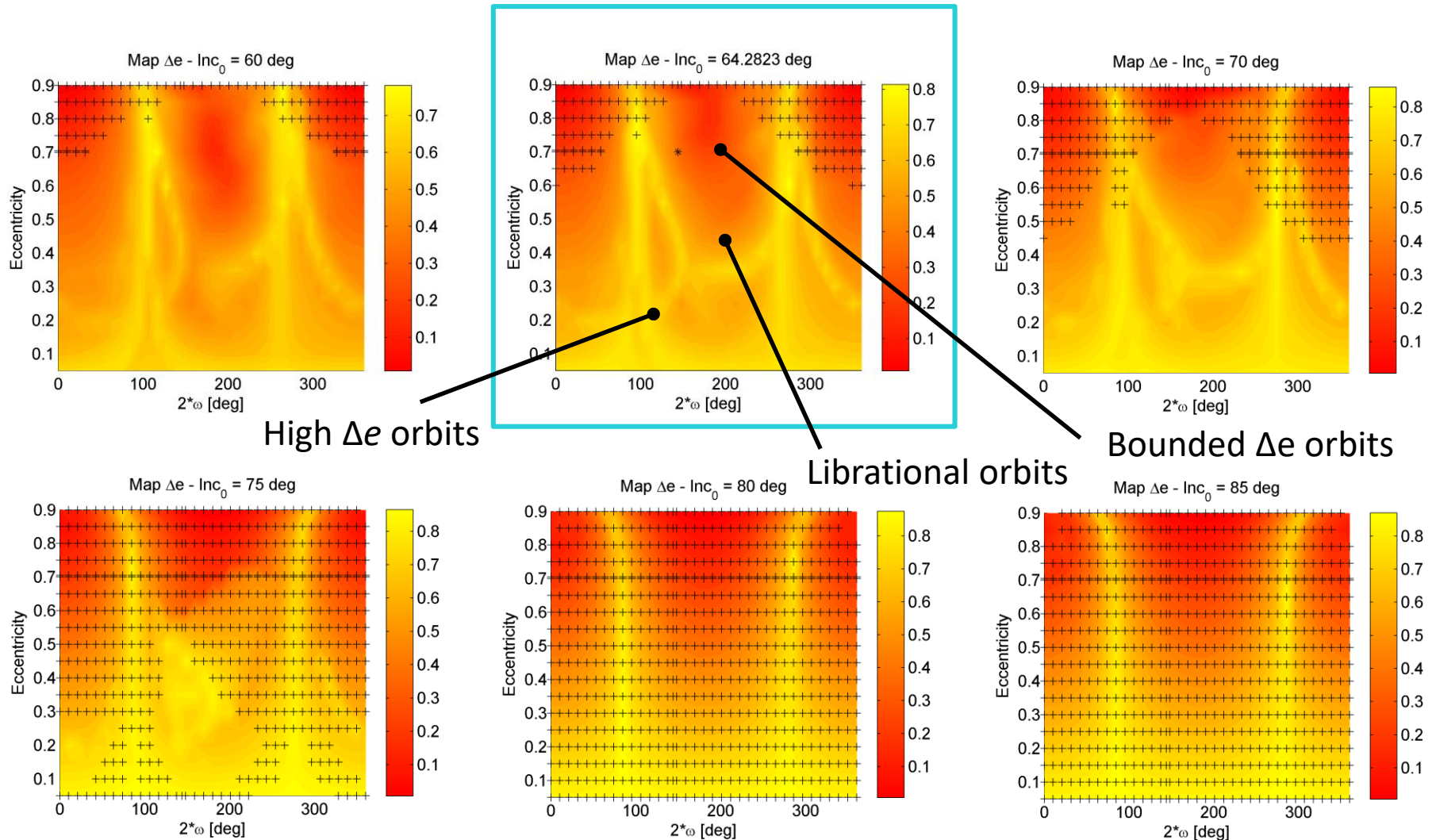
Dynamical maps

Long-term orbit evolution - Initial inclination 45 degrees



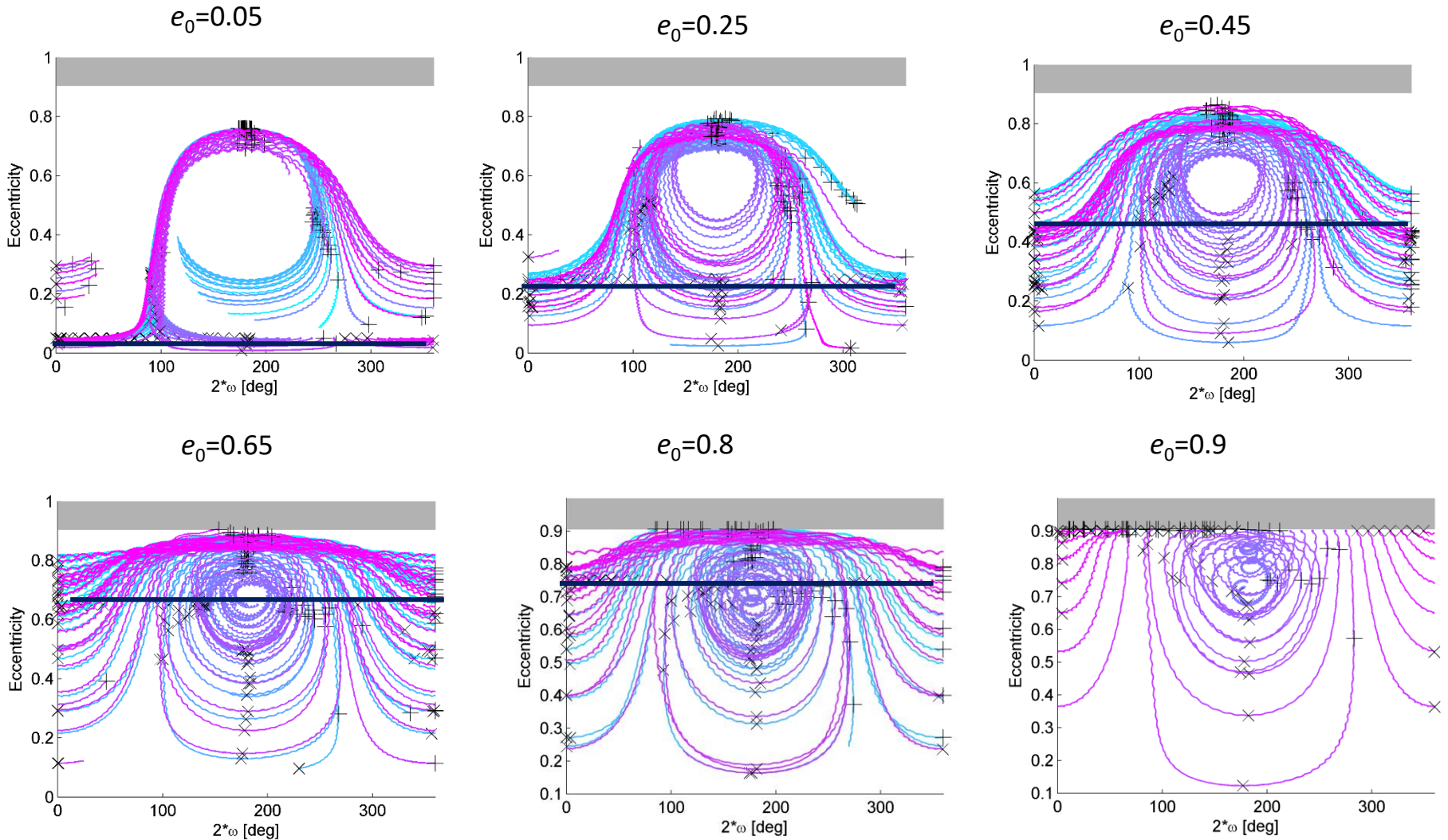
Dynamical maps

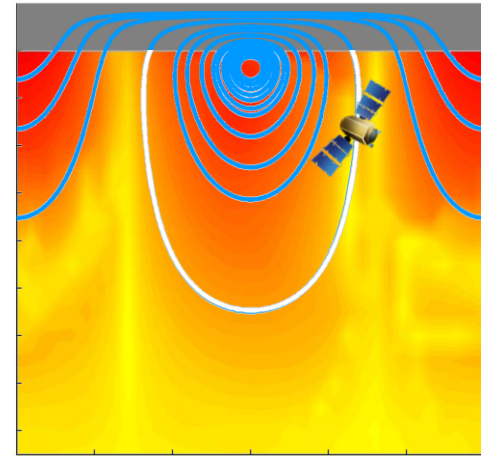
Long-term orbit evolution



Dynamical maps

Long-term orbit evolution - Initial inclination 64.28 degrees





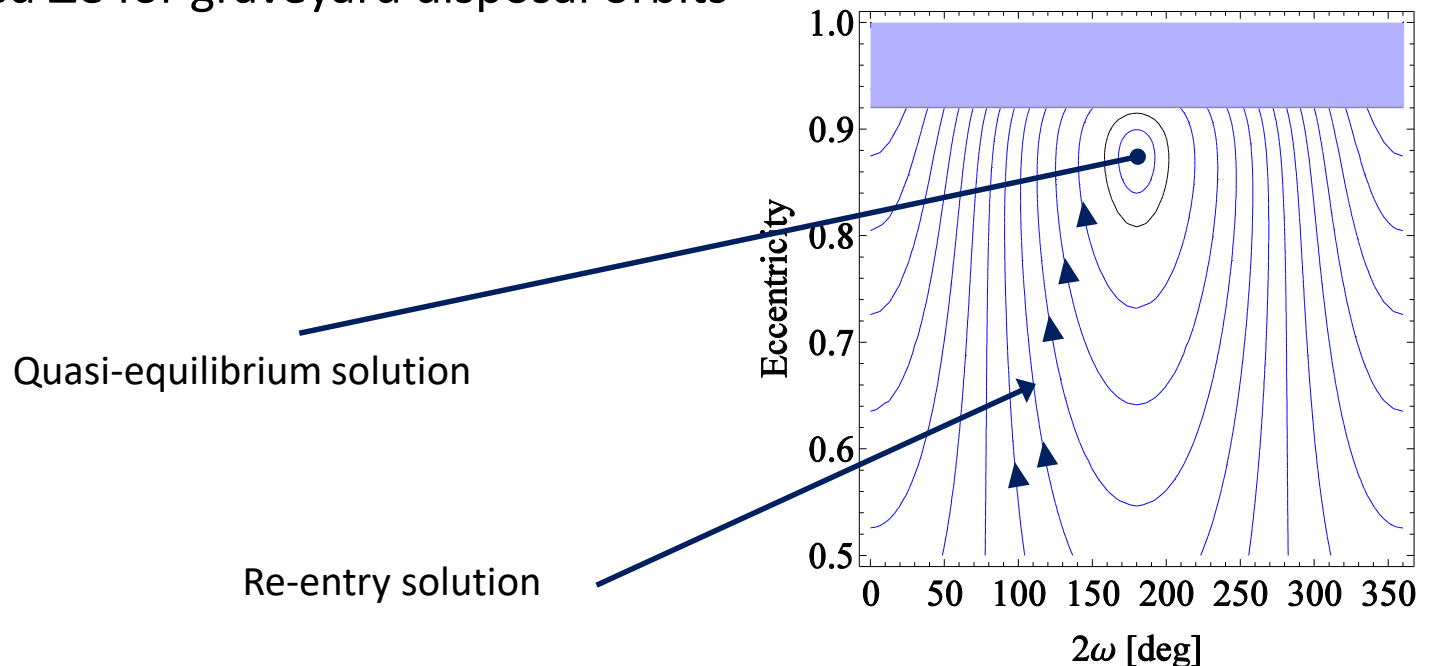
Design of disposal manoeuvres

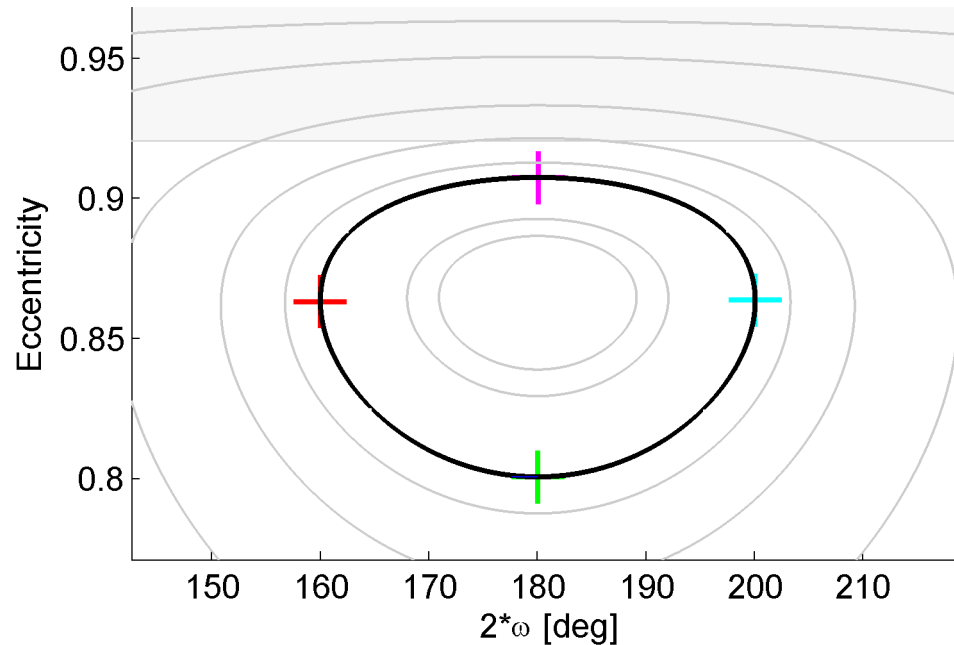
ENGINEERING PERTURBATION EFFECTS

Design disposal manoeuvre in the phase space

Design manoeuvre in the phase space

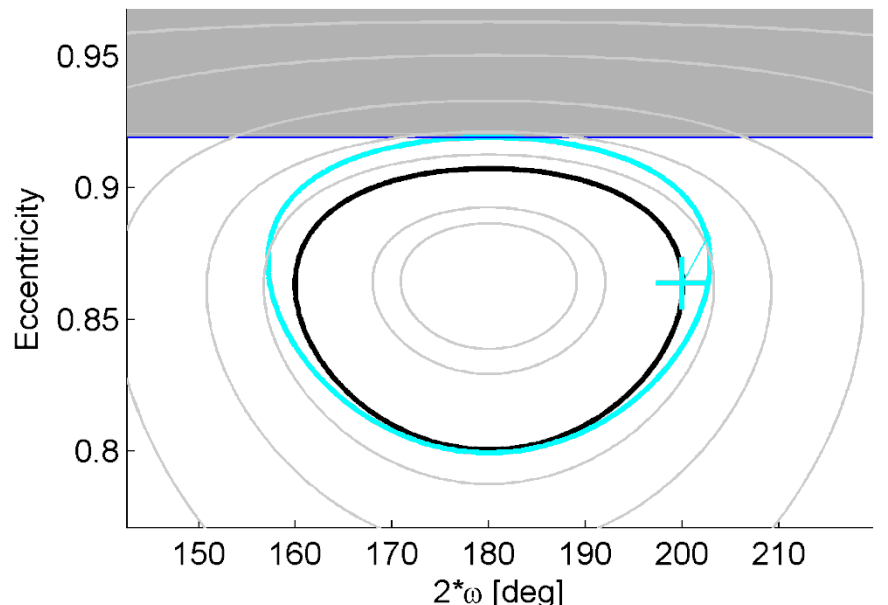
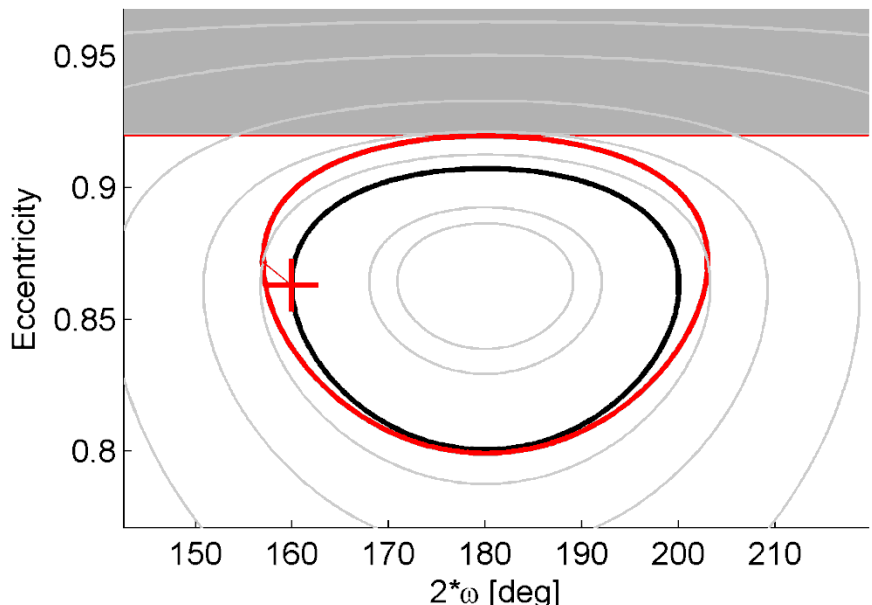
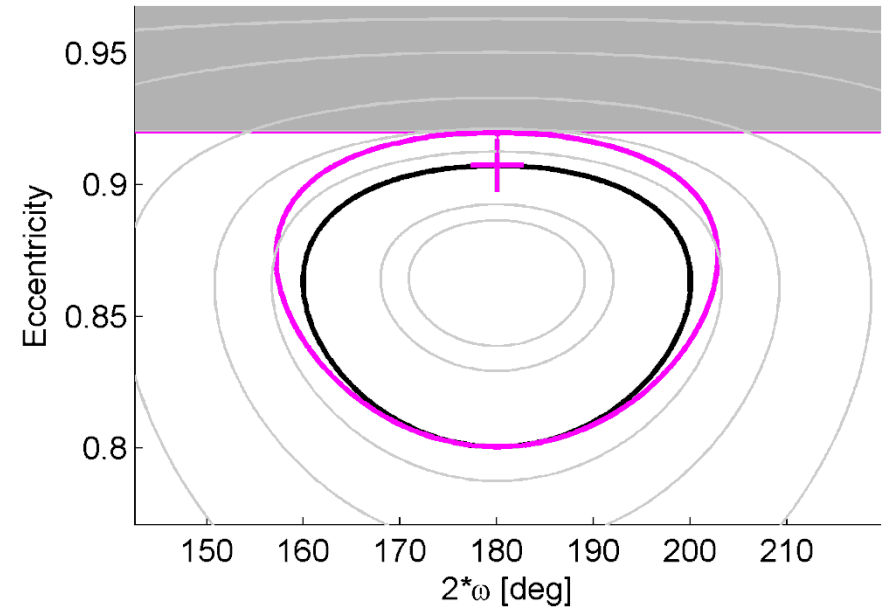
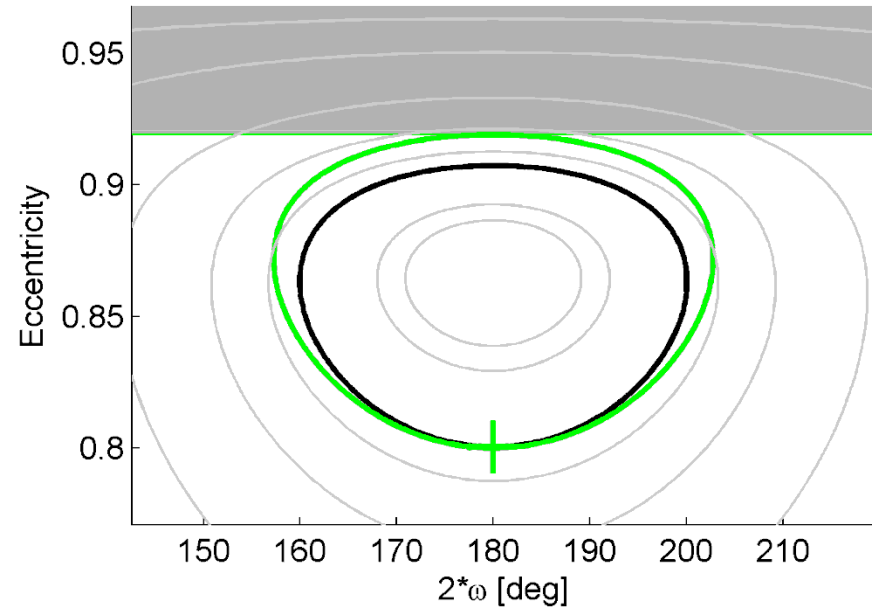
- Re-entry transfer on trajectories in the phase space to reach $e_{\text{crit}} = 1 - (R_{\text{Earth}} + h_{p, \text{drag}}) / a$
Maximum Δe exploitable for re-entry or free orbit change
- Graveyard: transfer to quasi-stable point in the phase space
Bounded Δe for graveyard disposal orbits





- Optimisation
$$\min_{\{\Delta v, \delta, \beta, f\}} \Delta v \quad C : \max [e(t)] = e_{\text{crit}}$$
- Multi-start method plus local constrained optimisation
- Gauss planetary eqs. for finite differences to compute change in orbital elements
- Orbit evolution computed with double average eqs.

Preliminary analysis Earth re-entry



Engineering the perturbation effects

Design disposal manoeuvre in the phase space

Single manoeuvre

$$\Delta \mathbf{v} = \Delta v \begin{bmatrix} \cos \alpha \cos \beta \\ \sin \alpha \cos \beta \\ \sin \beta \end{bmatrix}$$



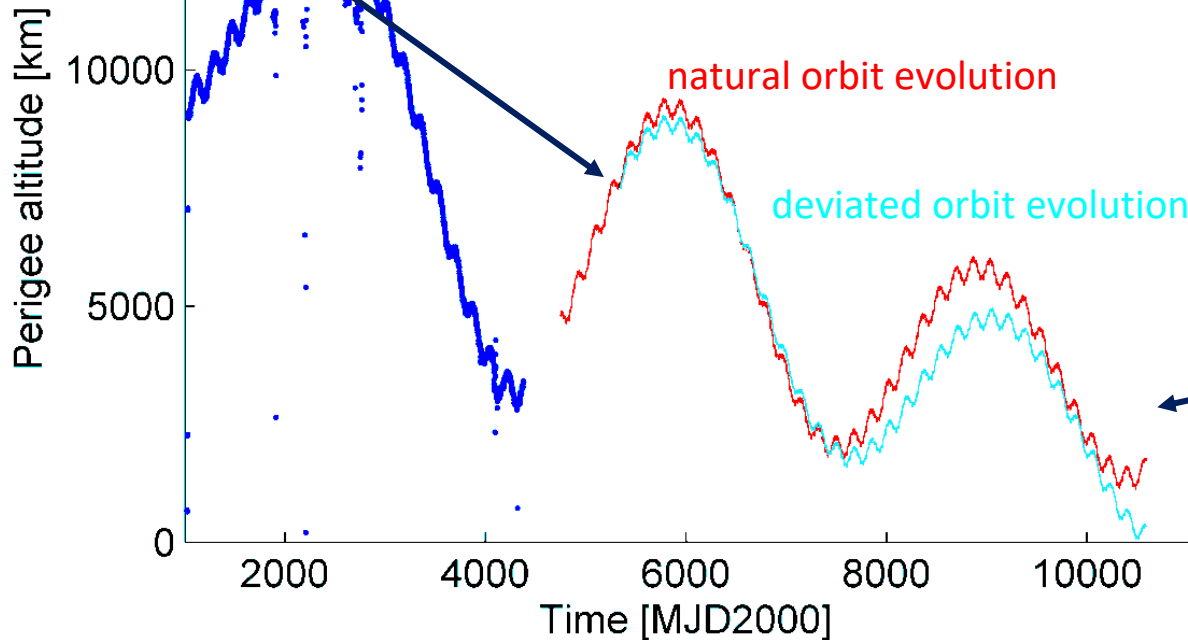
$$\Delta kep = G(kep(t_m), f_m, \Delta \mathbf{v})$$

Gauss' planetary equations in finite-difference form



$$kep_d = kep(t_m) + \Delta kep$$

Deviated condition



Minimum perigee within selected time interval for disposal

$$h_{p,\min} = \min_{t \in \Delta t_{\text{disposal}}} h_p(t)$$

► Colombo, Letizia, Alessi, Landgraf, 24th AAS/AIAA 2014



APPLICATIONS



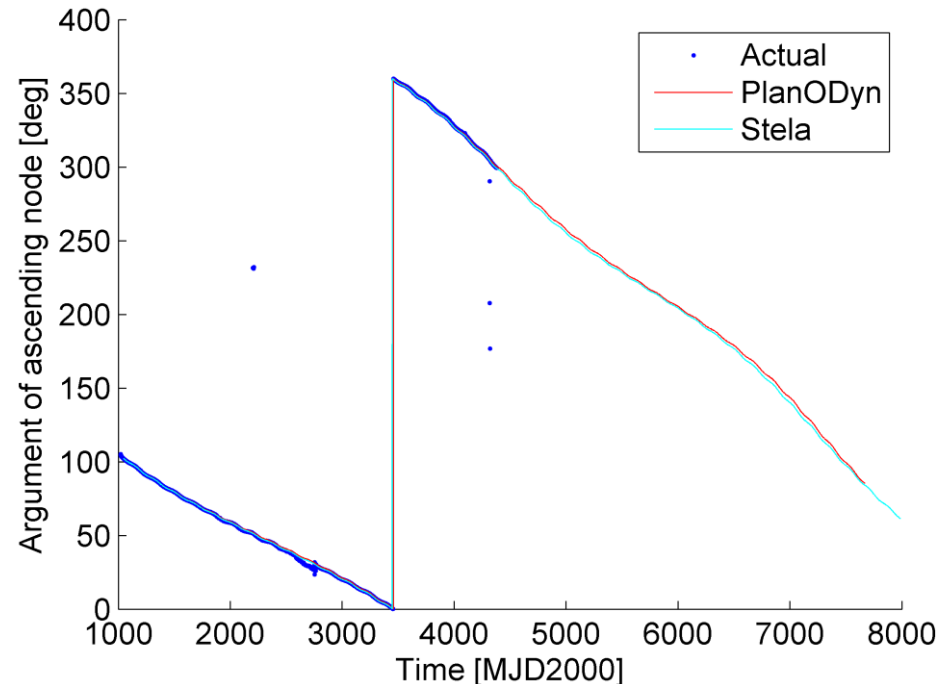
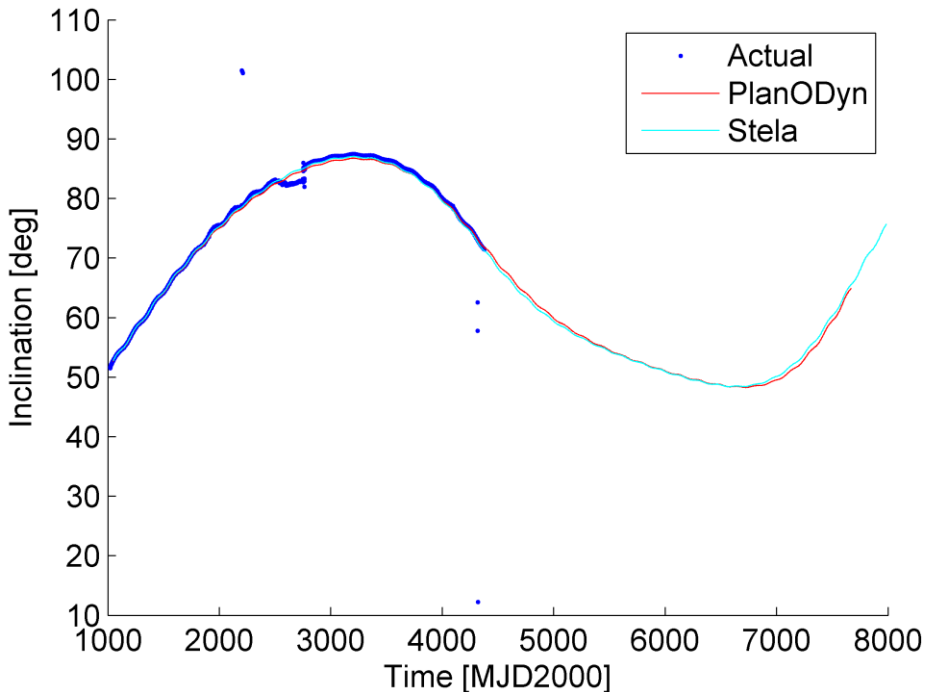
Integral: gamma-ray observatory

ESA's Integral observatory is able to detect gamma-ray bursts, the most energetic phenomena in the Universe

Operational orbit

Mission scenario

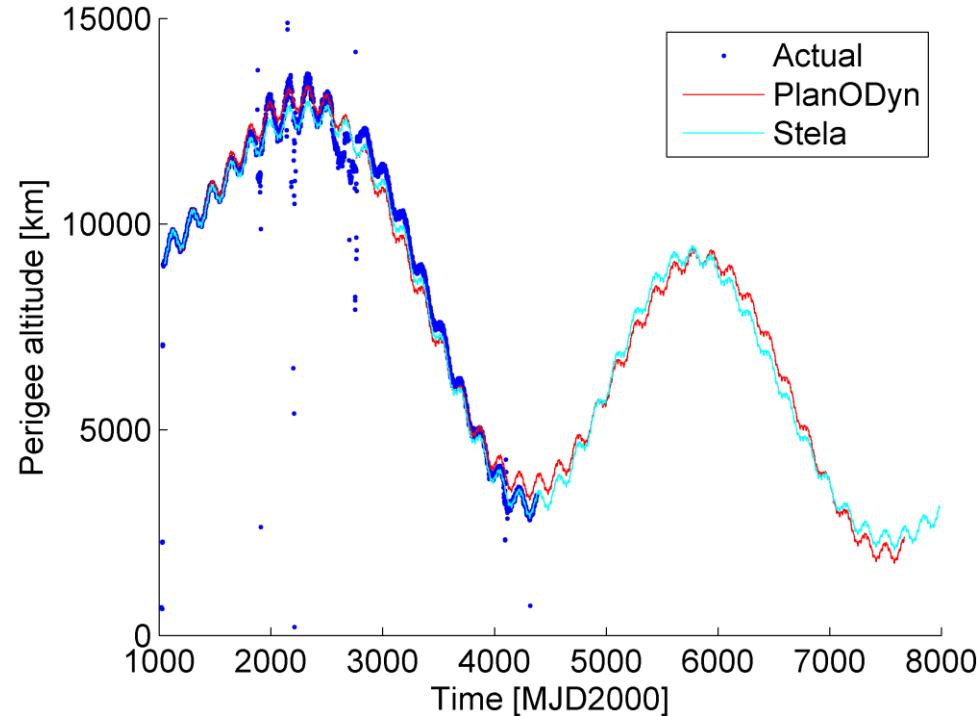
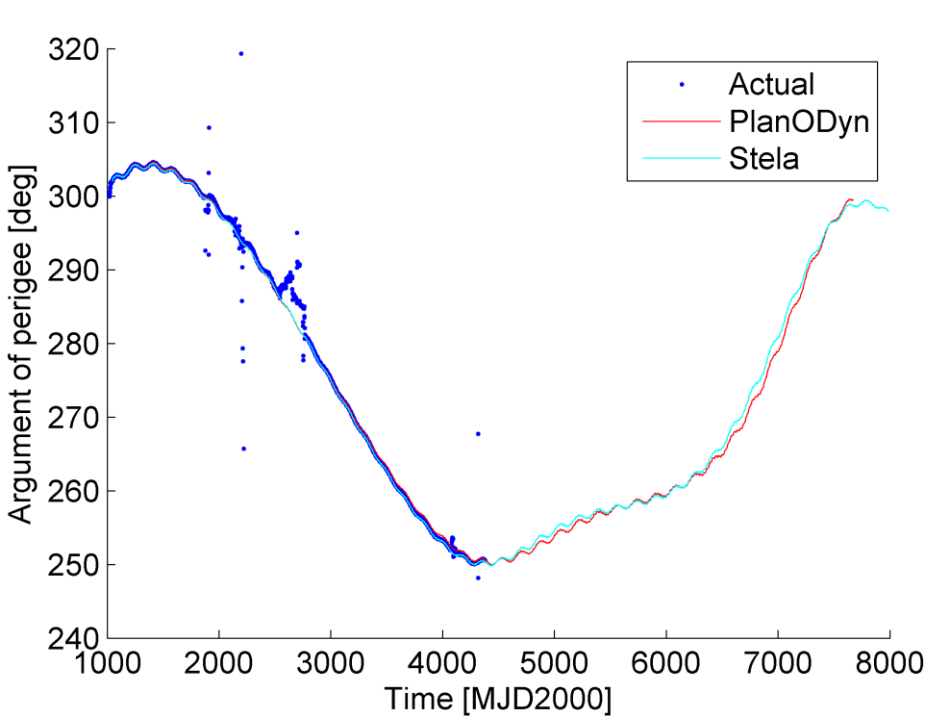
- Propagation time: 2002/11/13 to 2021/01/01
- Initial Keplerian elements from Horizon NASA on 2002/11/13 at 00:00:
 $a = 87736$ km, $e = 0.82403$, $i = 0.91939$ rad, $\Omega = 1.7843$ rad, $\omega = 5.271$ rad



Operational orbit

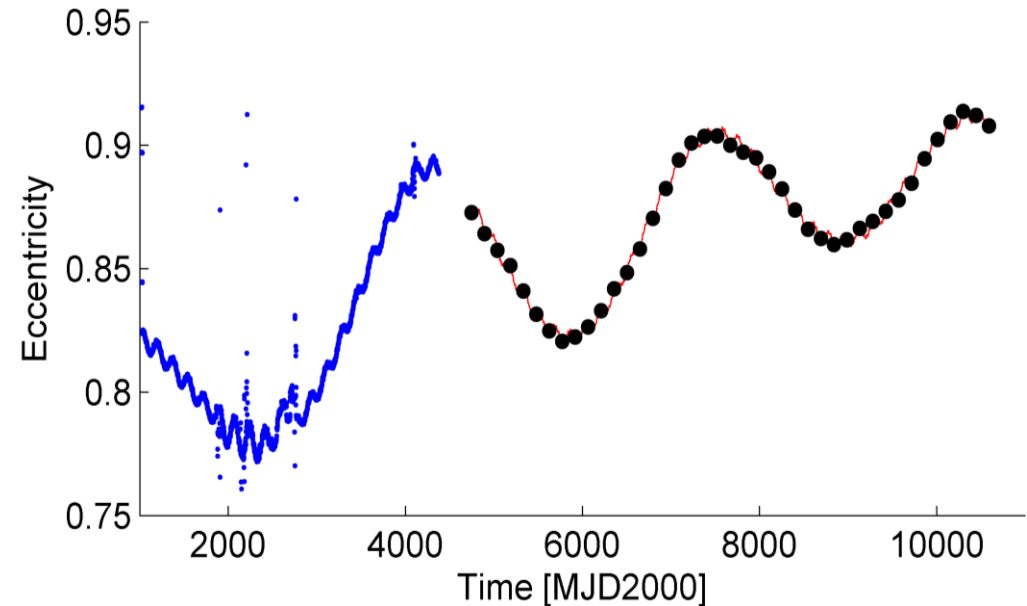
Mission scenario

- Propagation time: 2002/11/13 to 2021/01/01
- Initial Keplerian elements from Horizon NASA on 2002/11/13 at 00:00:
 $a = 87736$ km, $e = 0.82403$, $i = 0.91939$ rad, $\Omega = 1.7843$ rad, $\omega = 5.271$ rad



Design disposal manoeuvre in the phase space

- Only 5 Keplerian elements are propagated: a , e , i , Ω , ω
- Optimal true anomaly f_M where the manoeuvre is applied is selected through optimisation
- Dynamics of the mean/true anomaly is much faster than the evolution
- Single manoeuvre considered at different dates within a wide disposal window [2013/01/01 to 2029/01/01]



Re-entry disposal design

For each initial condition global optimization $x = [\Delta v \quad \alpha \quad \beta \quad f]$

$$J = \max(h_{p,\min} - h_{p,\text{target}}, 0)^2 + w \cdot \Delta v \quad \text{minimise } \Delta v$$

target minimum perigee

$$h_{p,\min} = \min_{t \in \Delta t_{\text{disposal}}} h_p(t) \qquad h_{p,\text{target}} = 50 \text{ km}$$

Genetic algorithm

- Population of 100 individuals and a maximum of 200 generations
- The tournament selection is applied to identify the best individuals and the mutation is used 10% of the times to maintain genetic diversity

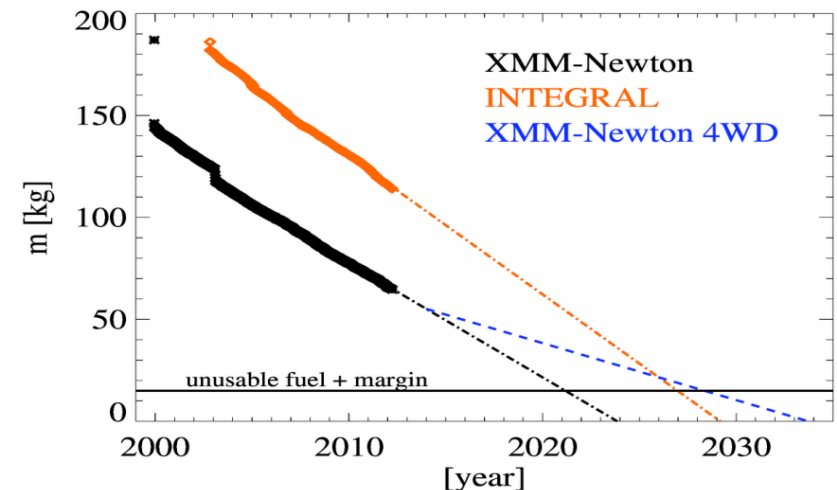
Constraints

Mission constraints

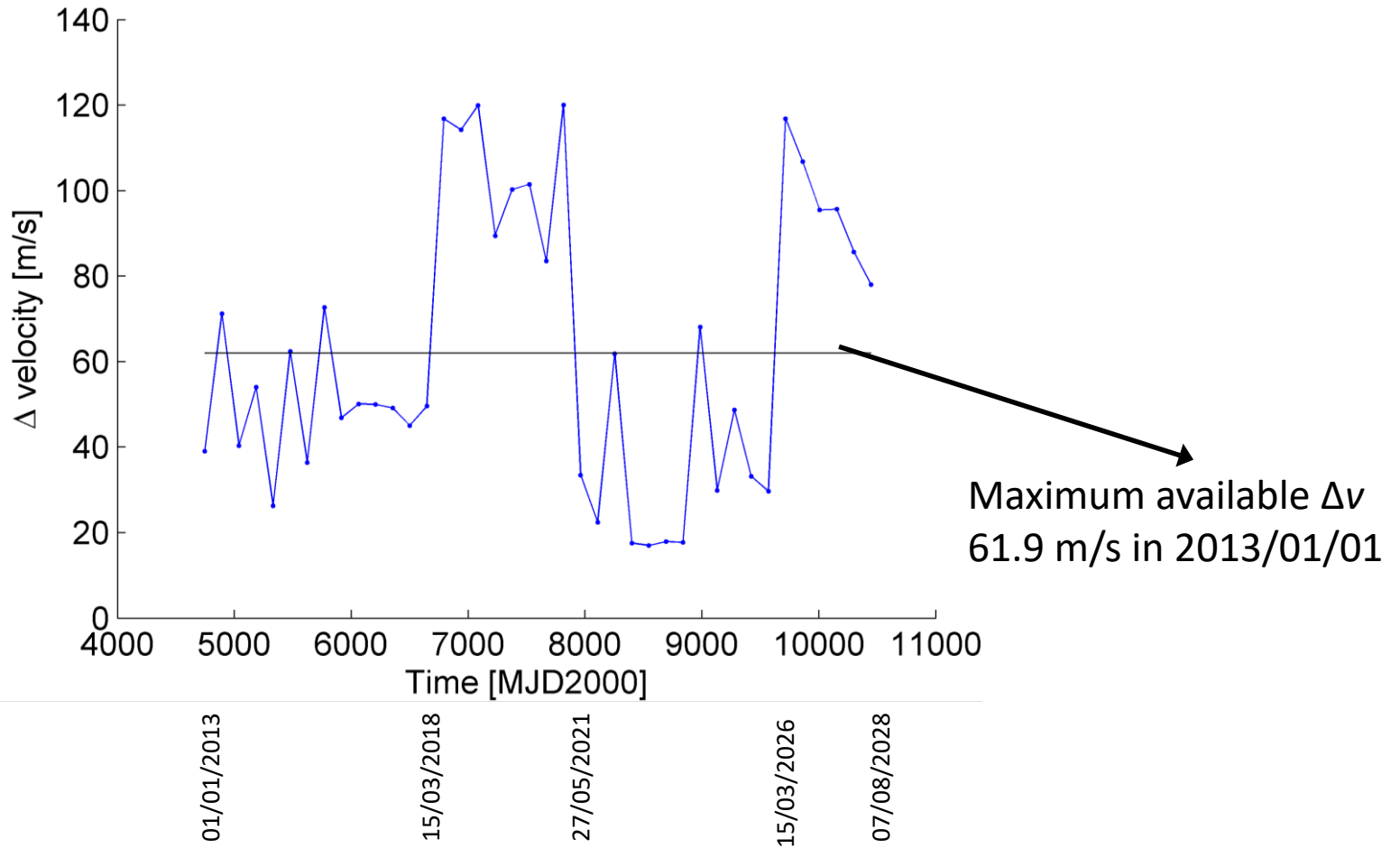
Parameter	Value
Dry mass	3414 kg
No. thrusters thrust	8 x 20 N
Specific impulse I_{sp}	235 s
Propellant	Hydrazine
Available fuel (01/01/2013)	61.5 kg
Equivalent Δv	61.9 m/s
Fuel consumption	8 kg/year
Pointing constraints	Telescope never points closer than 15 deg from the Sun
c_R at BOL	1.3
Max A/m EOL	0.013 m ² /kg

Mission extended

- Change in attitude and orbital control system (four reaction wheels instead of three nominal + one redundancy)
- Limiting the degradation of the wheels
- Reduction of the fuel consumption.
- Spacecraft lifetime would increase of 6-8 years (going from 2020 to 2026-2028)



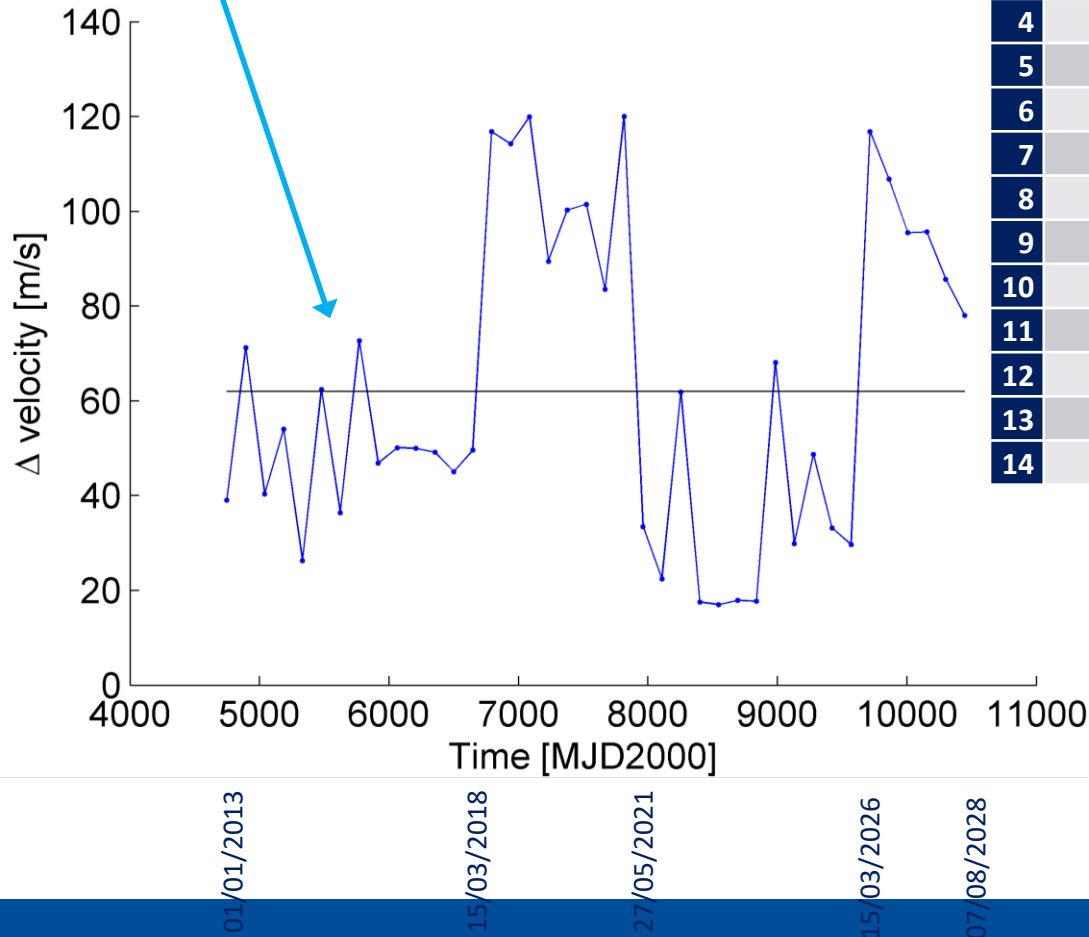
Results



Results

Family 1

re-entry in 2028, Δv between 27 and 73 m/s

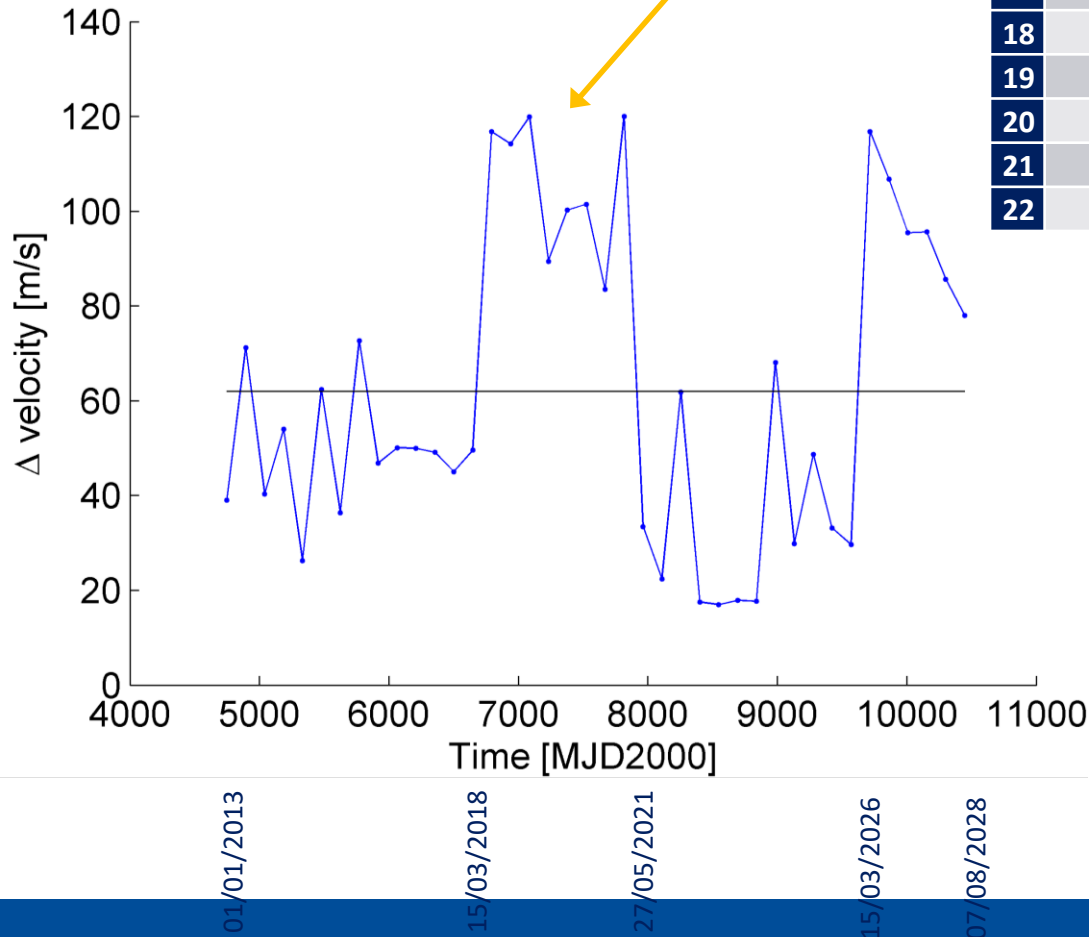


N	Re-entry manoeuvre [date]	Δv [m/s]	Re-entry epoch [date]	Minimum perigee [km]
1	01/01/2013	39.03	19/09/2028	49.86
2	27/05/2013	71.23	19/09/2028	49.72
3	20/10/2013	40.28	20/09/2028	49.21
4	15/03/2014	54.03	19/09/2028	49.72
5	08/08/2014	26.26	16/10/2028	49.99
6	01/01/2015	62.39	18/09/2028	49.62
7	27/05/2015	36.33	19/09/2028	49.10
8	20/10/2015	72.66	19/09/2028	50.33
9	14/03/2016	46.80	08/04/2028	49.56
10	07/08/2016	50.06	19/09/2028	49.83
11	01/01/2017	49.99	19/09/2028	49.03
12	27/05/2017	49.11	08/04/2028	49.04
13	20/10/2017	45.03	08/04/2028	46.25
14	15/03/2018	49.55	18/09/2028	49.82

INTEGRAL mission

Results

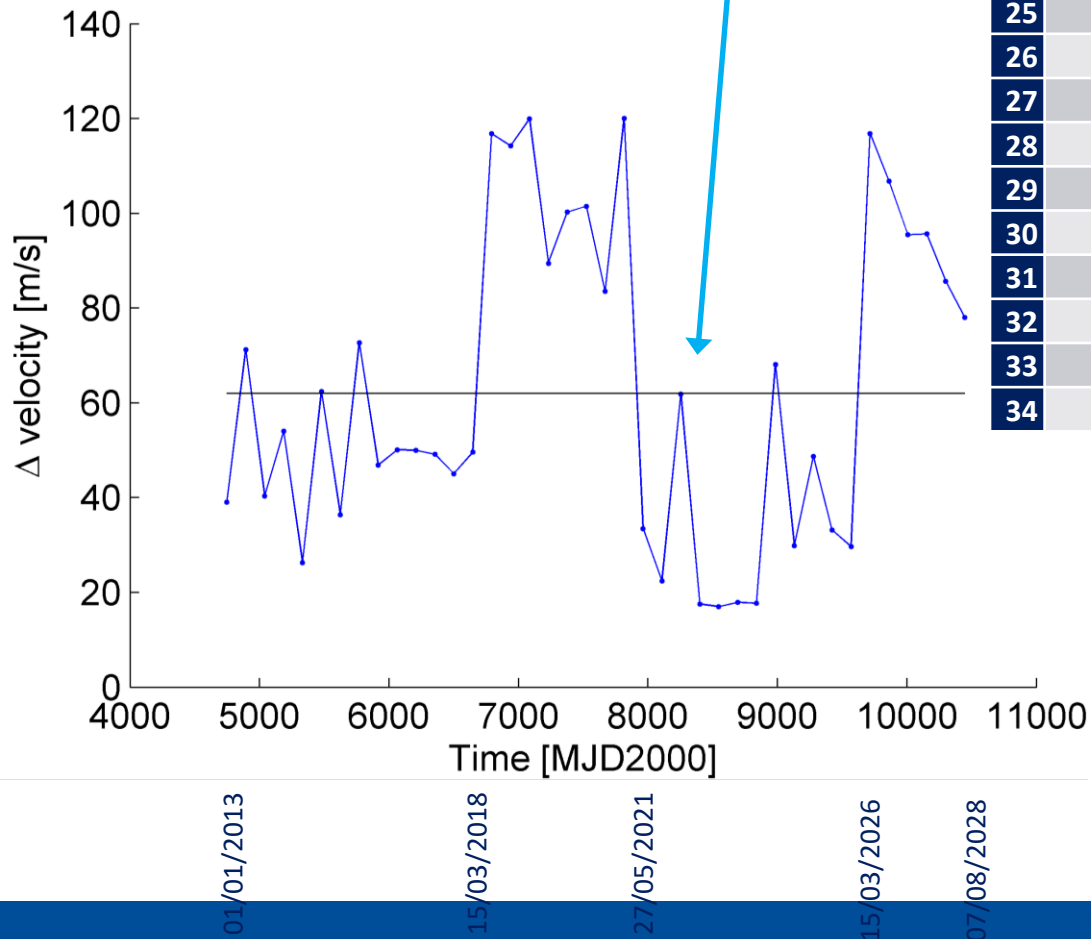
Family 2
reach minimum perigee
between 2019 and 2020
(quicker re-entry)



N	Re-entry manoeuvre [date]	Δv [m/s]	Re-entry epoch [date]	Minimum perigee [km]
15	08/08/2018	116.7488	18/10/2028	50.08
16	01/01/2019	114.23	14/10/2019	49.37
17	27/05/2019	119.89	09/11/2019	48.42
18	20/10/2019	89.40	17/10/2028	49.99
19	14/03/2020	100.26	22/04/2020	49.99
20	07/08/2020	101.48	02/10/2020	47.89
21	01/01/2021	83.48	19/09/2028	49.65
22	27/05/2021	120.02	13/09/2026	48.68

Results

Family 3
re-entry in 2028,
 Δv between 17 and 70 m/s

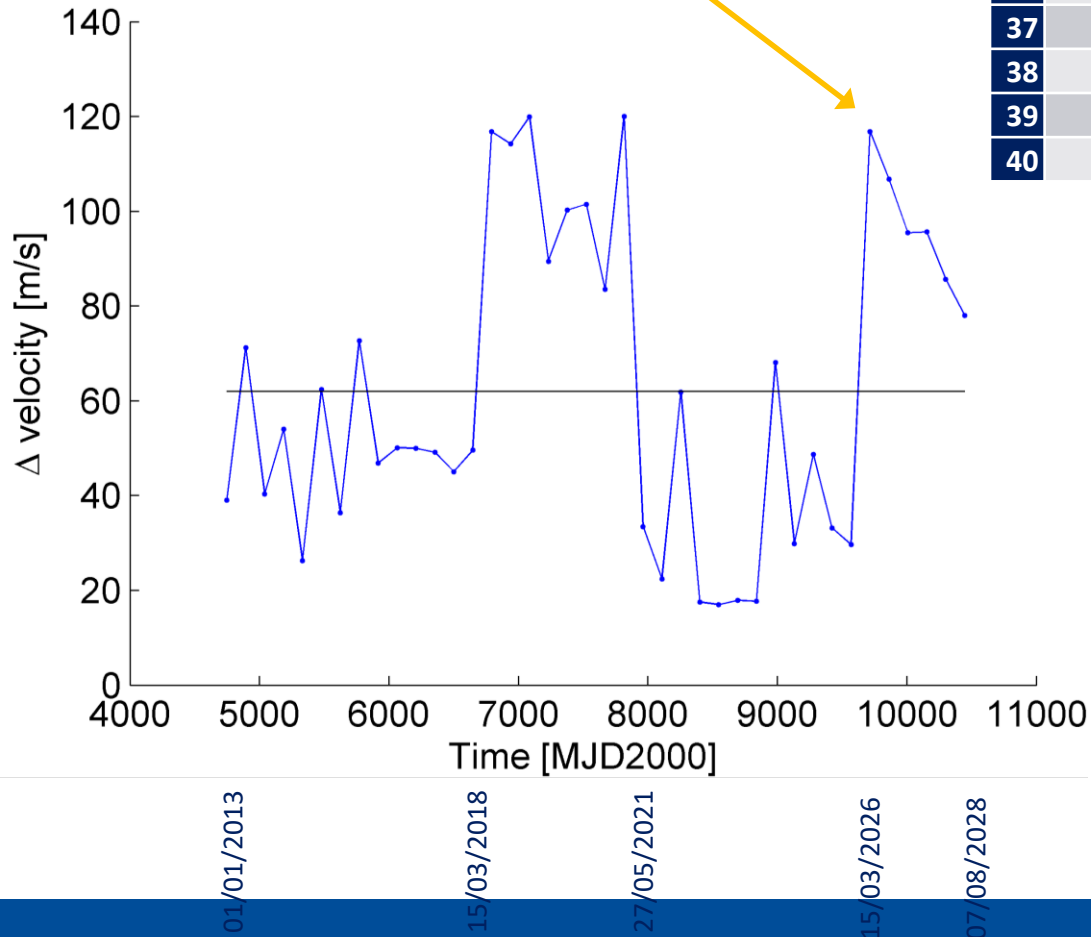


N	Re-entry manoeuvre [date]	Δv [m/s]	Re-entry epoch [date]	Minimum perigee [km]
23	20/10/2021	33.38	18/09/2028	48.24
24	15/03/2022	22.38	18/09/2028	45.53
25	08/08/2022	61.83	08/04/2028	49.84
26	01/01/2023	17.51	19/09/2028	46.46
27	27/05/2023	16.97	18/09/2028	49.71
28	20/10/2023	17.92	18/09/2028	46.13
29	14/03/2024	17.68	19/09/2028	45.28
30	07/08/2024	68.04	18/09/2028	49.94
31	01/01/2025	29.79	08/04/2028	48.81
32	27/05/2025	48.71	18/09/2028	39.33
33	20/10/2025	33.13	18/09/2028	28.31
34	15/03/2026	29.65	19/09/2028	49.09

Results

Family 4

have a quick re-entry in 2028 but requires higher Δv than family 3



N	Re-entry manoeuvre [date]	Δv [m/s]	Re-entry epoch [date]	Minimum perigee [km]
35	08/08/2026	116.78	20/04/2027	48.88
36	01/01/2027	106.77	22/04/2027	48.40
37	27/05/2027	95.43	02/10/2027	48.14
38	20/10/2027	95.60	12/03/2028	49.83
39	14/03/2028	85.58	08/04/2028	48.47
40	07/08/2028	78.04	18/09/2028	48.78

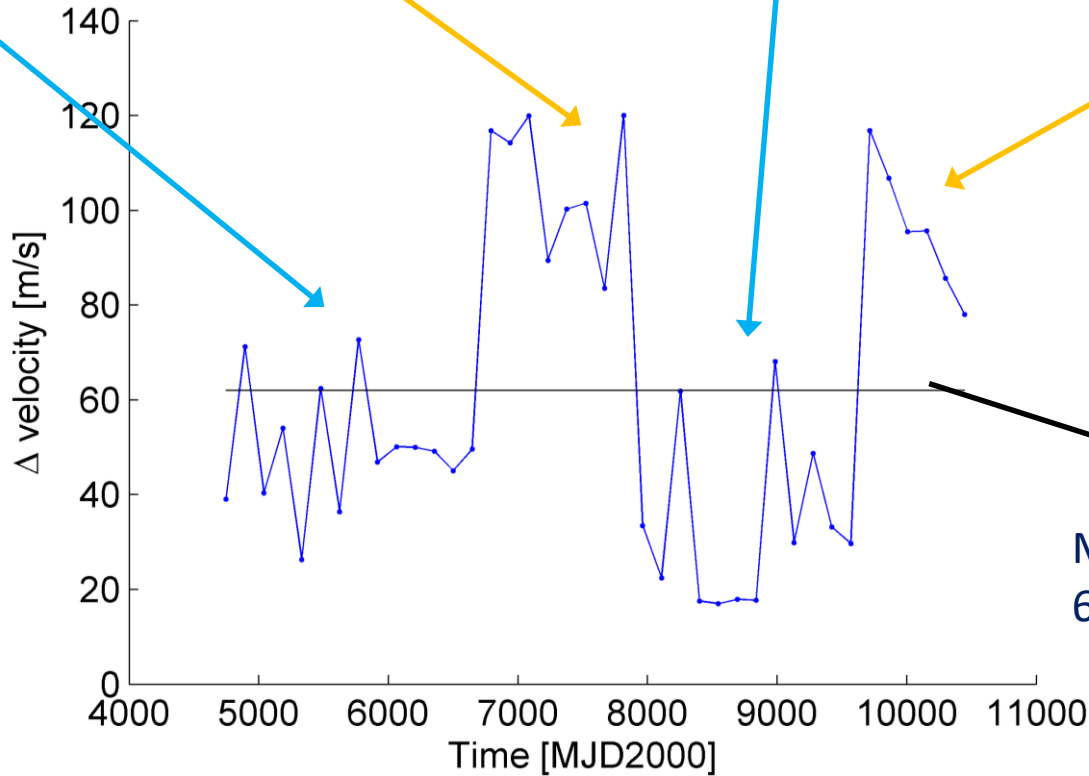
INTEGRAL mission

Family 1
re-entry in 2028, Δv
between 27 and 73
m/s

Family 2
reach minimum perigee
between 2019 and 2020
(quicker re-entry)

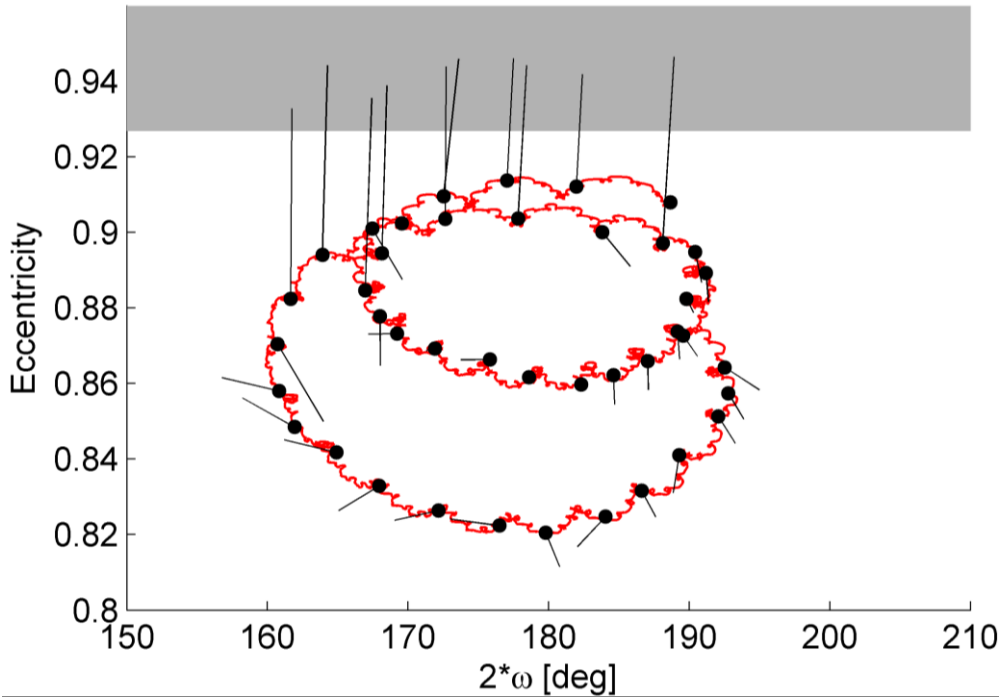
Family 3
re-entry in 2028, Δv
between 17 and 70
m/s

Family 4
have a quick re-entry in
2028 but requires higher Δv
than family 3



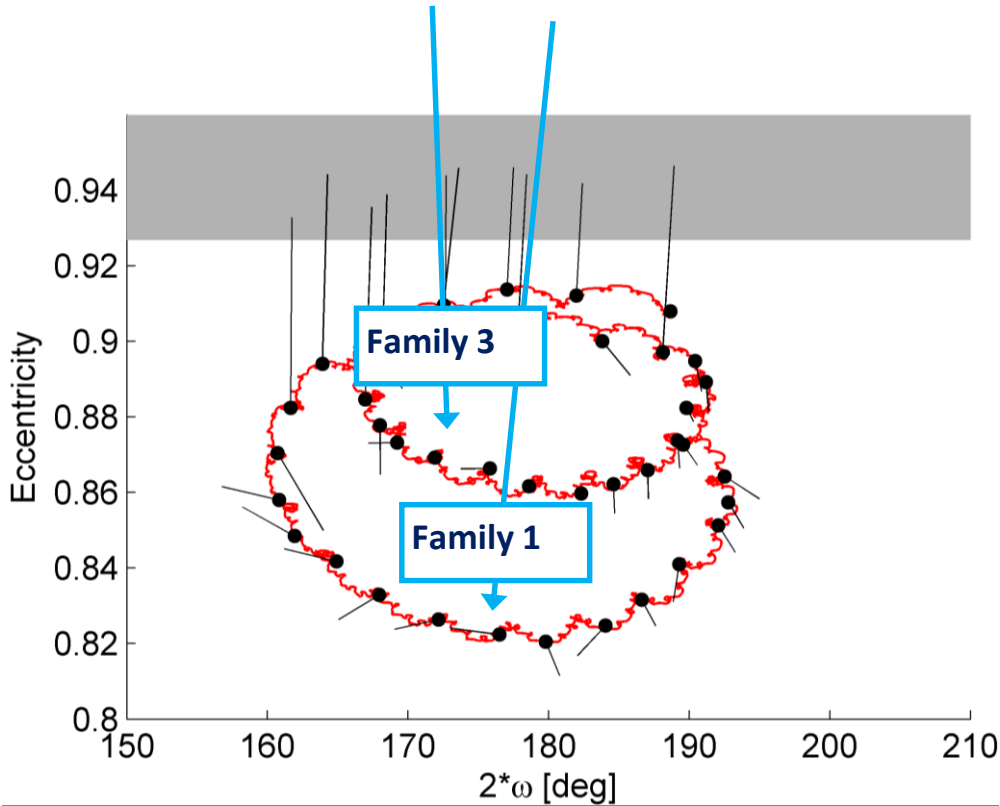
Maximum available Δv
61.9 m/s in 2013/01/01

Results



Results

Low eccentricity conditions



Results

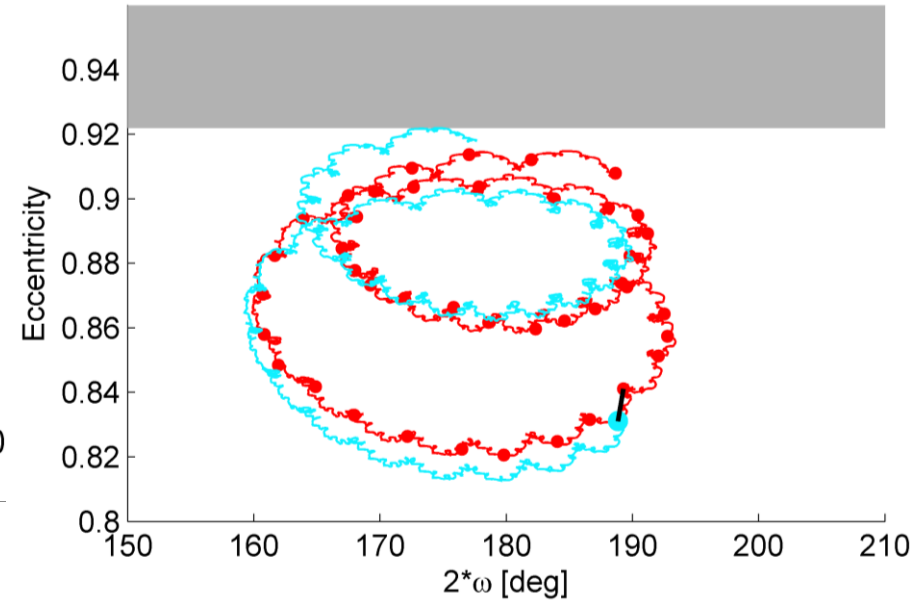
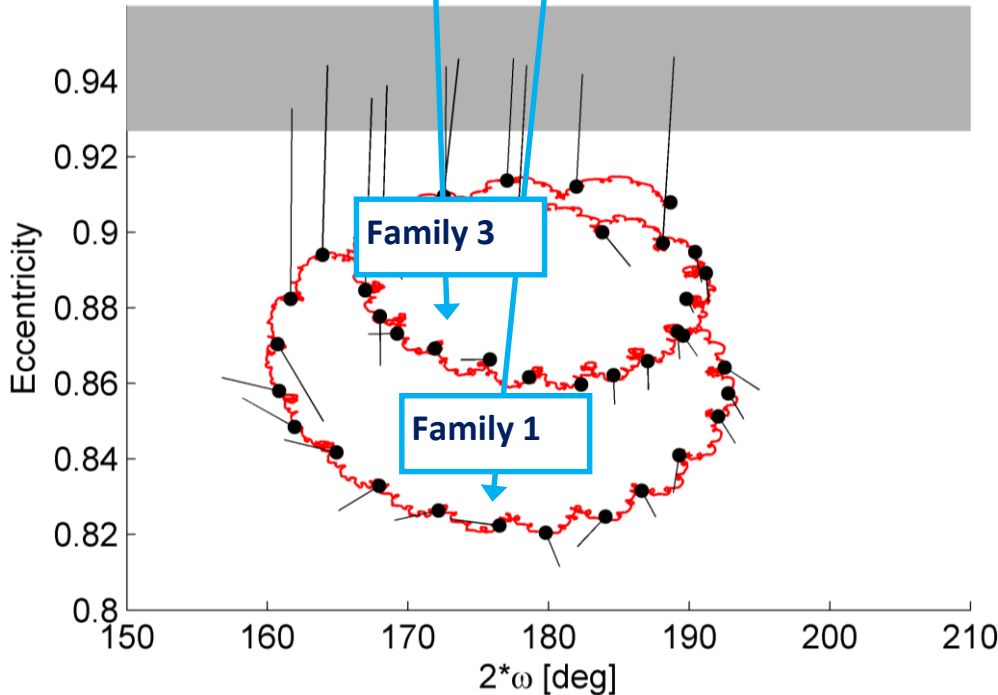
Low eccentricity conditions
Manoeuvre performed on 08/08/2014
Re-entry in 2028



The manoeuvre tends to further decrease e

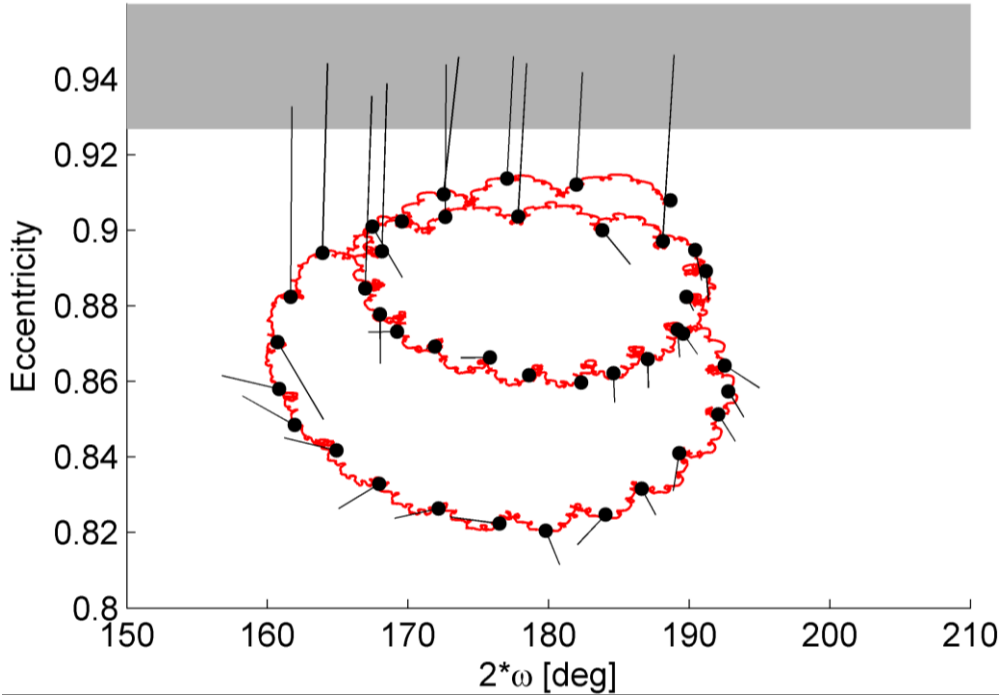
→ the following long term propagation will reach a higher eccentricity (re-entry).

The manoeuvre is more efficient (i.e., lower Δv is required).



INTEGRAL mission

Results

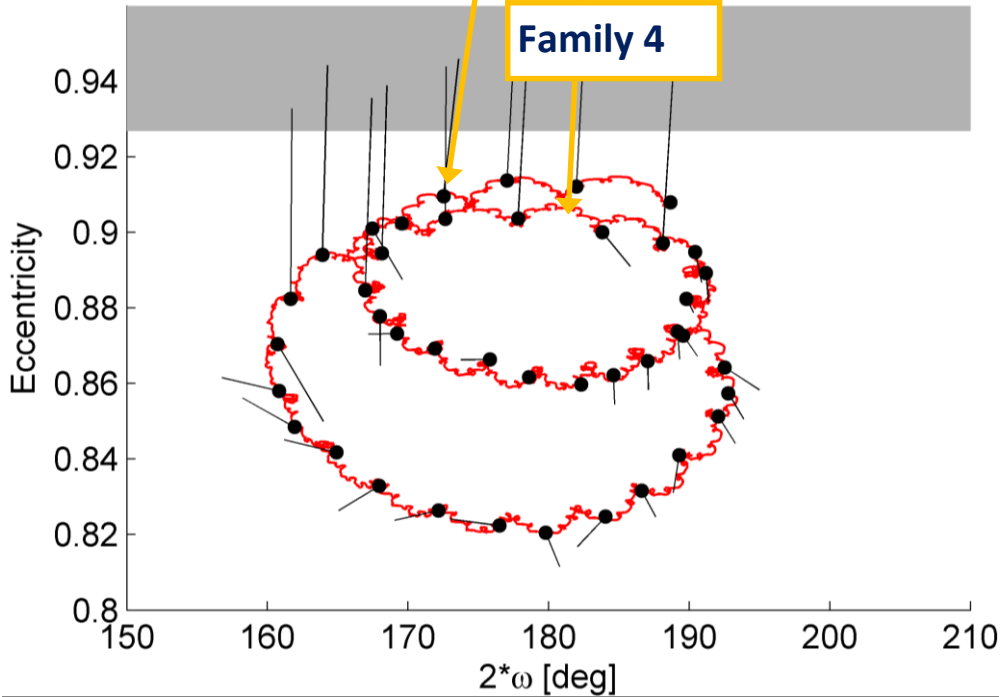


Results

High eccentricity conditions

Family 2

Family 4

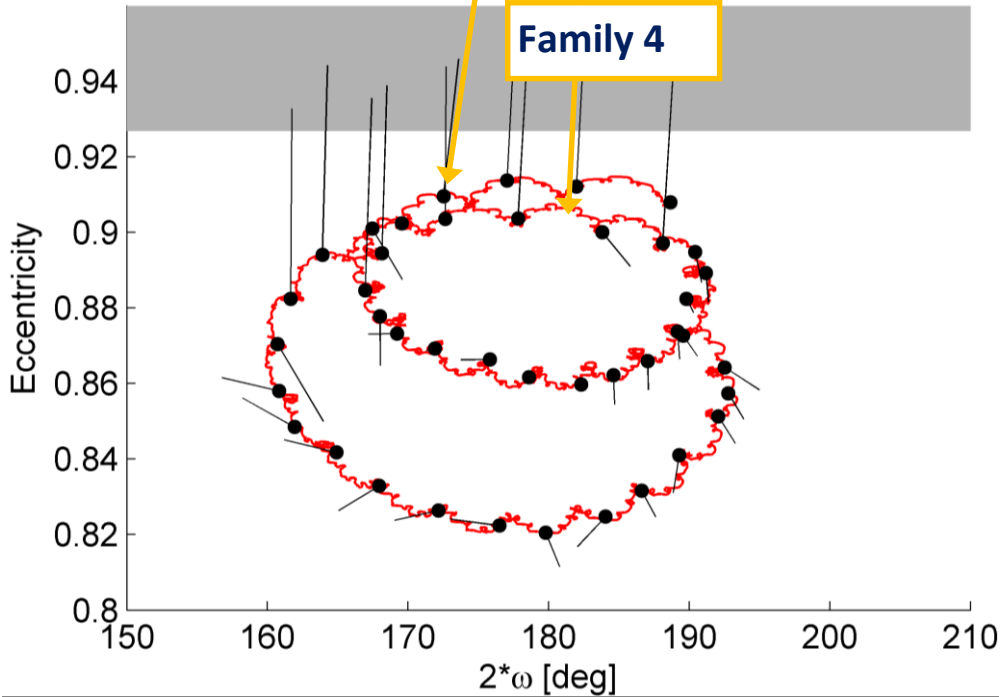


Results

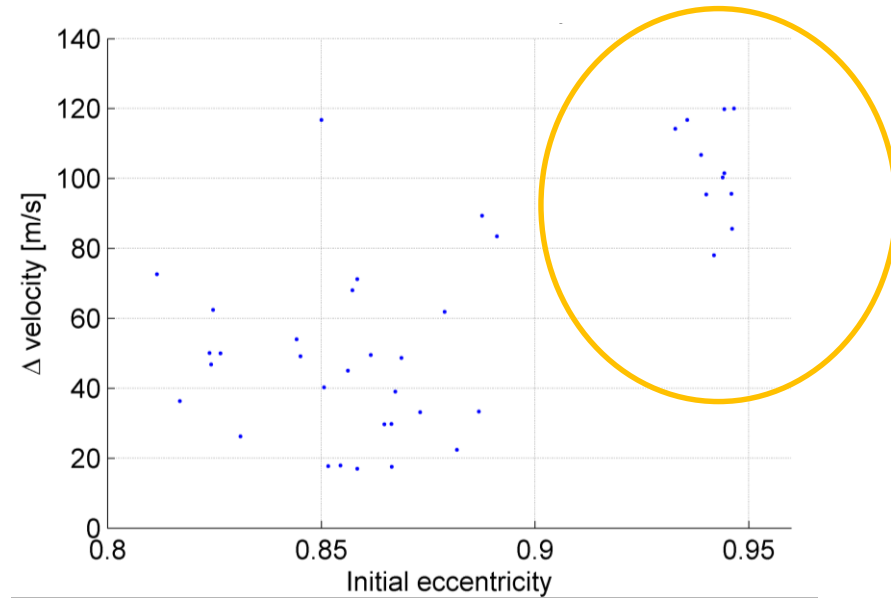
High eccentricity conditions

Family 2

Family 4



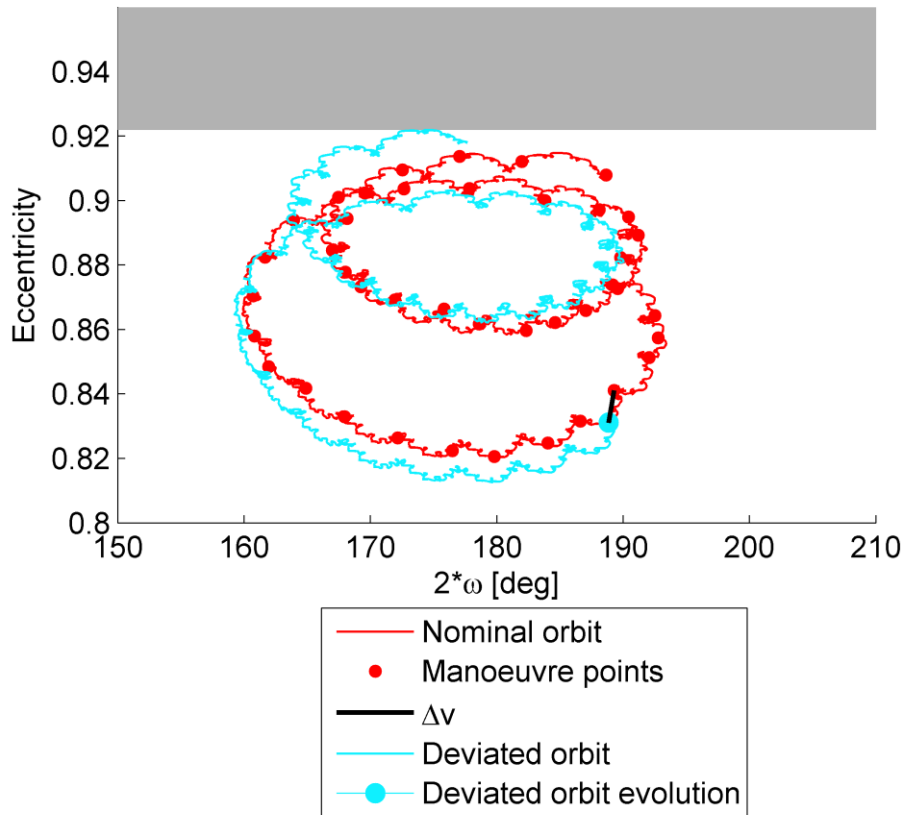
The re-entry manoeuvre aims at further increasing the eccentricity, so that the target minimum perigee is reached after a relatively shorter time



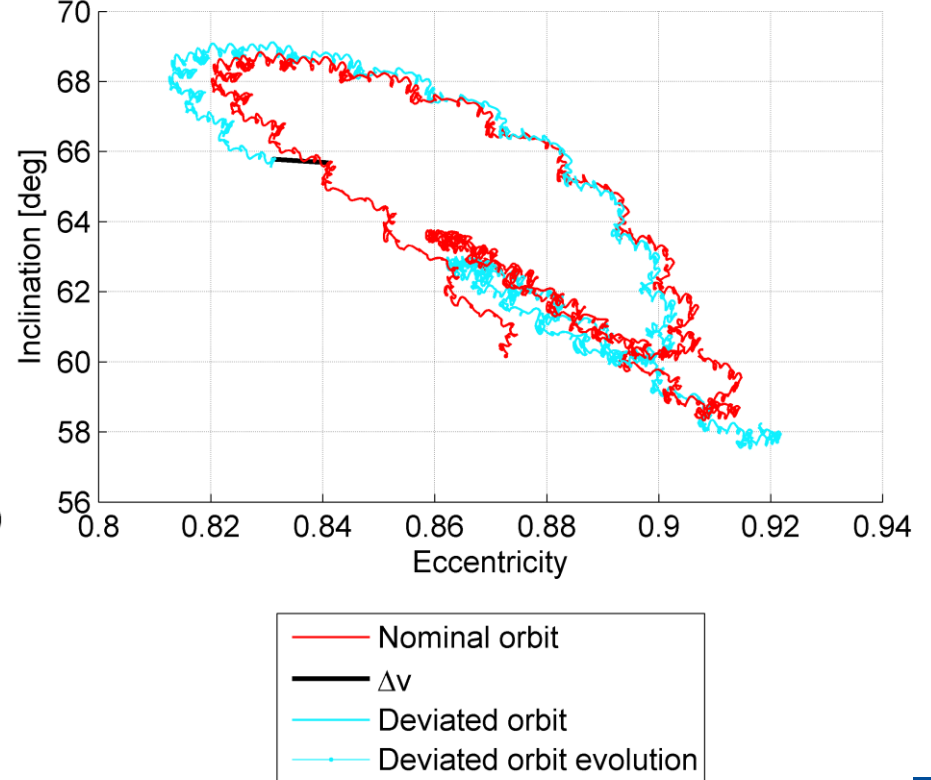
Re-entry manoeuvre

Example: manoeuvre performed on 08/08/2014

INTEGRAL, System: @Earth Earth-Moon plane

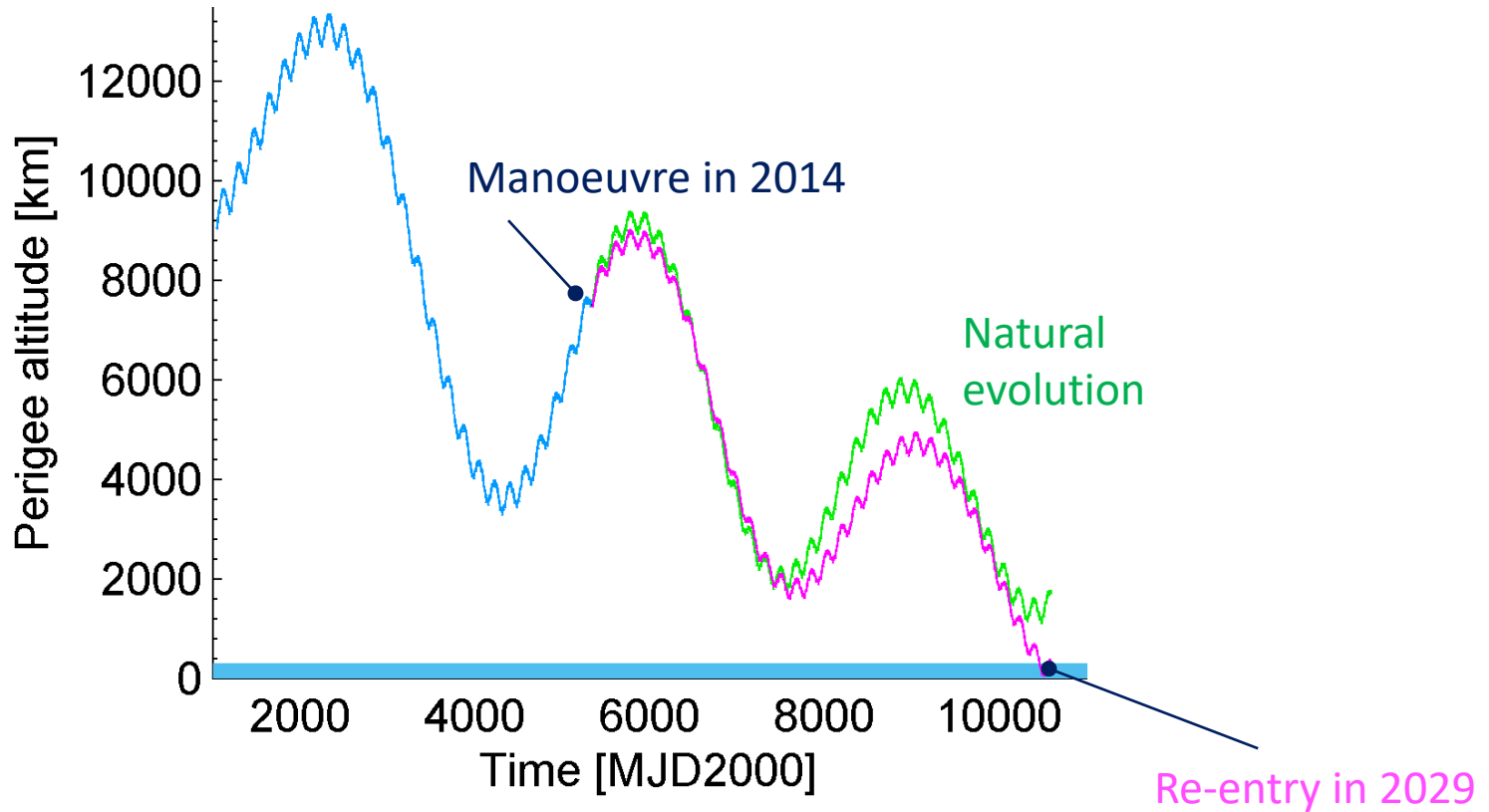


INTEGRAL, System: @Earth Earth-Moon plane



INTEGRAL mission

Re-entry manoeuvre

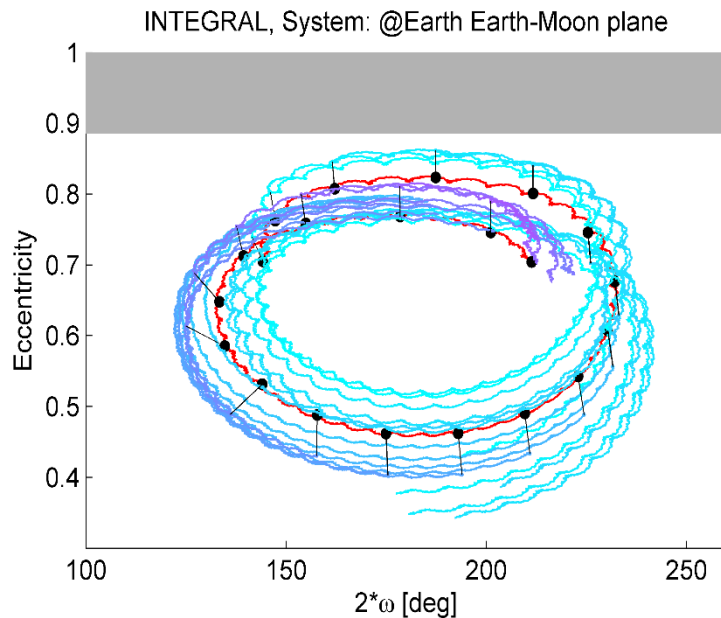


Graveyard disposal

- Time window for starting the disposal manoeuvre [2013/01/01 to 2035/01/01].
- Max Δv available for the manoeuvre 81 m/s

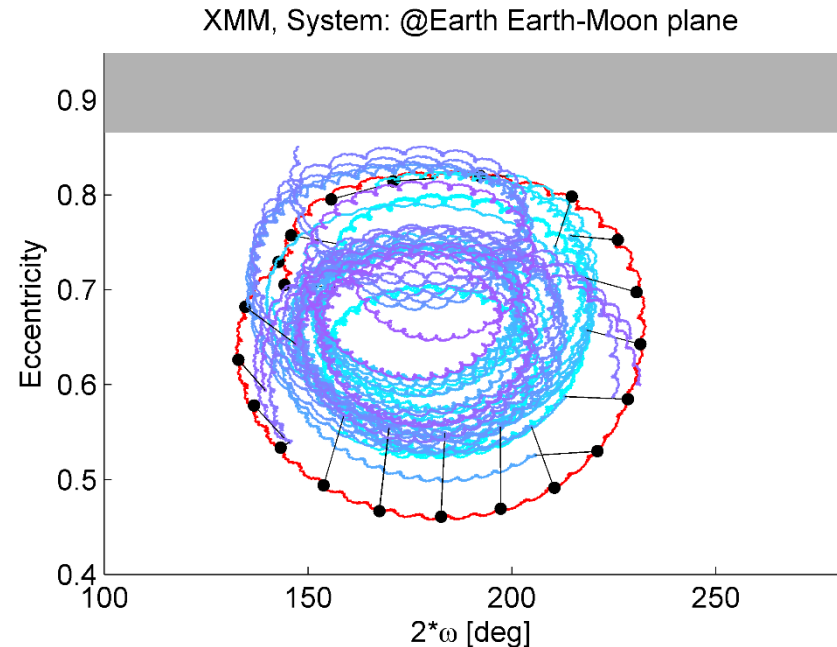
Re-entry

Max Δe , min h_p orbits



Graveyard

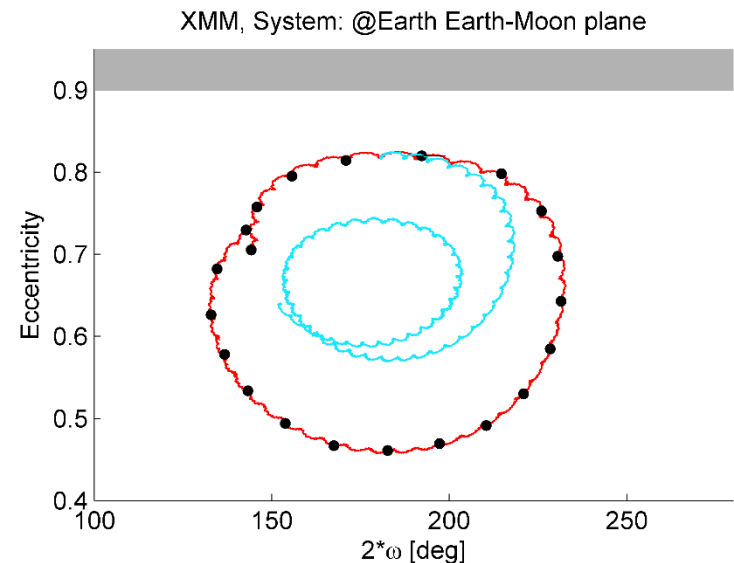
Limited Δe , Δi orbits



Graveyard disposal

- Time window for starting the disposal manoeuvre [2013/01/01 to 2035/01/01].
- Max Δv available for the manoeuvre 81 m/s

Example graveyard maneuver
performed on 20/04/2016





CONCLUSIONS

- Effect of luni-solar perturbations and the Earth's oblateness on the stability of highly elliptical orbits
- Natural orbital dynamics can be exploited and enhanced
- INTEGRAL is the demonstration in Space!



INTEGRAL REVOLUTION
1799

INTEGRAL CURRENT TARGET
Galactic Center

Integral Target and Scheduling Information

Schedule: **All executed** **Current revolution (1799)** Future schedule

Revolution 1799 to 1799

Show... show pl

Schedule for revolution 1799

(this list is also available in csv-format, click [here](#) to download)

Rev	Start time (UTC)	End time (UTC)	Exp. time (s)	Target	Ra (J2000)	Dec (J2000)	Pattern	PI	Proposal	Observation	N
1799	2017-03-30 10:11:09	2017-03-30 13:52:56	12600	Gal. Bulge region	17:45:36.00	-28:56:00.0	HEX	Erik Kuulkers	1420001	1420001 / 0009	P
1799	2017-03-30 14:11:52	2017-03-30 14:45:12	2000	Galactic Center	17:36:47.26	-31:25:52.3	5x5 Seg	Joern Wilms	1420009	1420009 / 0001	
1799	2017-03-30 15:06:03	2017-03-31 05:48:09	50000	Galactic Center	17:35:00.58	-32:37:41.9	5x5 Seg	Joern Wilms	1420009	1420009 / 0005	
1799	2017-03-31 06:08:30	2017-03-31 09:50:16	12600	Galaxy (l=0, b=0)	17:41:53.52	-29:13:22.8	HEX	Rashid Sunyaev	1420021	1420021 / 0009	
1799	2017-03-31 10:50:17	2017-03-31 11:52:13	3600	Galaxy (l=0, b=-30)	19:58:20.40	-40:46:37.2	HEX	Rashid Sunyaev	1420021	1420021 / 0010	
1799	2017-03-31 12:27:37	2017-03-31 15:05:31	9000	Galaxy (l=0, b=-30)	19:58:20.40	-40:46:37.2	HEX	Rashid Sunyaev	1420021	1420021 / 0010	
1799	2017-03-31 15:33:09	2017-03-31 19:14:56	12600	Galaxy (l=0, b=0)	17:47:59.52	-30:08:27.6	HEX	Rashid Sunyaev	1420021	1420021 / 0011	
1799	2017-03-31 19:42:29	2017-03-31 23:24:15	12600	Galaxy (l=0, b=-30)	20:06:37.68	-41:09:50.4	HEX	Rashid Sunyaev	1420021	1420021 / 0012	

ReDSHIFT – H2020

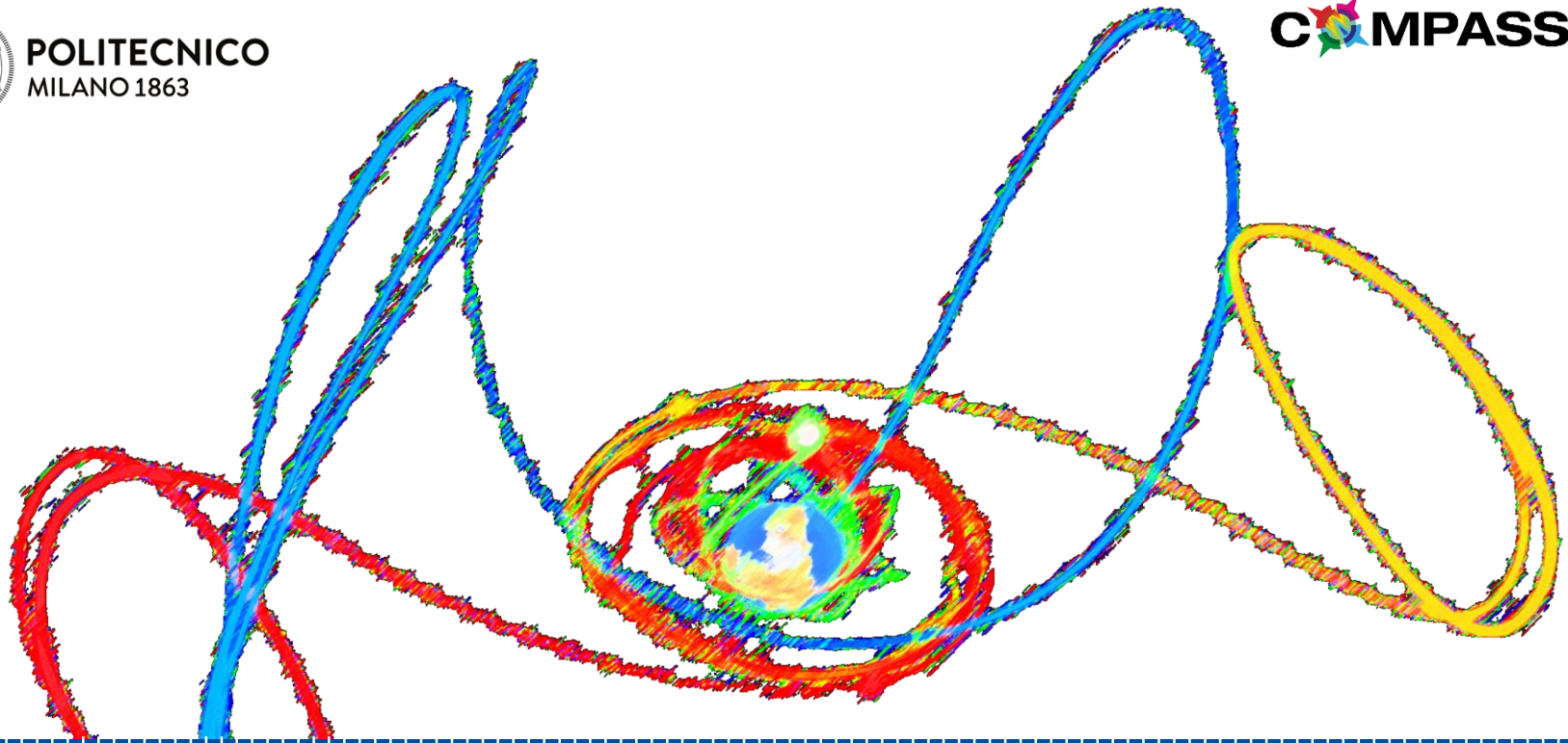
- Compute maps for the whole LEO to GEO environment
- Stability maps
- Disposal design for current and future s/c
- Online software
- See effect on global debris population

COMPASS- ERC

- Develop autonomous tool that exploit natural dynamics
- Study planetary protection requirements/uncertainties
- To be applied to debris cloud fragmentation, re-entry prediction, multi-moon mission, highly perturbed orbits (e.g. around asteroids)



POLITECNICO
MILANO 1863



Luni-solar perturbations for missions design in highly elliptical orbits

Camilla Colombo

CNES HEO workshop 31 March 2017